Developmental Biology 384 (2013) 166–180

Contents lists available at ScienceDirect

Developmental Biology

journal homepage: www.elsevier.com/locate/developmentalbiology

Small heat shock proteins are necessary for heart migration and laterality determination in zebrafish

Jamie L. Lahvic [a,1], Yongchang Ji [b], Paloma Marin [a], Jonah P. Zuflacht [a,2], Mark W. Springel [a,3], Jonathan E. Wosen [a], Leigh Davis [a,4], Lara D. Hutson [a,5], Jeffrey D. Amack [b], Martha J. Marvin [a,*]

[a] Williams College Department of Biology, 59 Lab Campus Drive, Williamstown, MA 01267, USA
[b] Department of Cell and Developmental Biology, State University of New York, Upstate Medical University, Syracuse, NY 13210, USA

ARTICLE INFO

Article history:
Received 19 March 2013
Received in revised form
4 October 2013
Accepted 7 October 2013
Available online 17 October 2013

Keywords:
Left–right asymmetry
Small heat shock protein
Cardia bifida
Kupffer's vesicle
Cilia
Yolk syncytial layer

ABSTRACT

Small heat shock proteins (sHsps) regulate cellular functions not only under stress, but also during normal development, when they are expressed in organ-specific patterns. Here we demonstrate that two small heat shock proteins expressed in embryonic zebrafish heart, *hspb7* and *hspb12*, have roles in the development of left–right asymmetry. In zebrafish, laterality is determined by the motility of cilia in Kupffer's vesicle (KV), where *hspb7* is expressed; knockdown of *hspb7* causes laterality defects by disrupting the motility of these cilia. In embryos with reduced *hspb7*, the axonemes of KV cilia have a 9+0 structure, while control embyros have a predominately 9+2 structure. Reduction of either *hspb7* or *hspb12* alters the expression pattern of genes that propagate the signals that establish left–right asymmetry: the *nodal*-related gene *southpaw* (*spaw*) in the lateral plate mesoderm, and its downstream targets *pitx2*, *lefty1* and *lefty2*. Partial depletion of *hspb7* causes concordant heart, brain and visceral laterality defects, indicating that loss of KV cilia motility leads to coordinated but randomized laterality. Reducing *hspb12* leads to similar alterations in the expression of downstream laterality genes, but at a lower penetrance. Simultaneous reduction of *hspb7* and *hspb12* randomizes heart, brain and visceral laterality, suggesting that these two genes have partially redundant functions in the establishment of left–right asymmetry. In addition, both *hspb7* and *hspb12* are expressed in the precardiac mesoderm and in the yolk syncytial layer, which supports the migration and fusion of mesodermal cardiac precursors. In embryos in which the reduction of *hspb7* or *hspb12* was limited to the yolk, migration defects predominated, suggesting that the yolk expression of these genes rather than heart expression is responsible for the migration defects.

Introduction

The small heat shock proteins (sHsps) are a phylogenetically ancient family that is represented in all kingdoms of life (Sun and MacRae, 2005). The sHsp family is defined by a conserved, approximately 80 amino acid alpha-crystallin protein binding domain, flanked by divergent carboxy- and amino-terminal regions. The sHsps were first recognized as low molecular weight chaperones that prevent aggregation of denatured proteins (Sun and MacRae, 2005). However selected members of the family have diverse functions beyond classically defined chaperone activity. Some sHsps regulate cytoskeleton assembly or associate with myofibrils (Fujita et al., 2004; Golenhofen et al., 2004; Houck and Clark, 2010; Krief et al., 1999; Tucker and Shelden, 2009).

Nine of the 13 zebrafish sHsps are expressed in temporal- and organ-specific patterns (Elicker and Hutson, 2007). Three sHsps, *hspb1* (*hsp27*), *hspb7* and *hspb12*, are expressed in the ventricle, atrioventricular canal (AVC) and outflow tract of the heart (Marvin et al., 2008) at 24–48 hpf (Marvin et al., 2008). In contrast to *hspb1*, which is ubiquitously expressed until 12 hpf and is upregulated by heat shock, *hspb7* and *hspb12* are expressed specifically in heart and skeletal muscle and their transcription is unaffected by heat shock (Marvin et al., 2008).

* Corresponding author. Fax: +1 413 597 3495.
E-mail address: mmarvin@williams.edu (M.J. Marvin).
[1] Present address: Stem Cell Program and Division of Hematology/Oncology and Harvard Stem Cell Institute, Harvard Medical School, Boston Children's Hospital, Boston, MA 02115, USA.
[2] Present address: Columbia University, College of Physicians and Surgeons, New York, NY 10032.
[3] Present address: Department of Pathology, Boston Children's Hospital, Boston, MA 02115, USA.
[4] Present address: University of Pennsylvania Veterinary School, Philadelphia, PA 19104, USA.
[5] Present address: Department of Biological Sciences, University at Buffalo, Buffalo, NY 14260, USA.

0012-1606/$ - see front matter © 2013 Elsevier Inc. All rights reserved.
http://dx.doi.org/10.1016/j.ydbio.2013.10.009

Human HSPB7 (cvHsp) is primarily localized to the cardiovascular system and skeletal muscle, and is upregulated by disease and age (Doran et al., 2007, 2006). Genome-wide association studies link mutations in HSPB7 to dilated cardiomyopathy (Matkovich et al., 2010; Stark et al., 2010). HSPB7 inhibits aggregation of poly-glutamine proteins but lacks chaperone activity (Vos et al., 2010). *hspb12* is found only in birds and fish and is most closely related to *hspb7*; however there is little homology between the two proteins outside the conserved α-crystallin domain (Elicker and Hutson, 2007). Remarkably, although *hspb1* is dispensable for normal heart development in zebrafish (Tucker et al., 2009), reduction of *hspb1* in *Xenopus* causes cardia bifida (Brown et al., 2007).

Asymmetry of the internal organs is a universal characteristic of vertebrate development and is critically important for normal embryogenesis. The establishment of left–right asymmetry proceeds in three main phases; the breaking of symmetry relative to the other axes, the initiation and expansion of the asymmetric gene expression cascade, and the interpretation of laterality signals by the organs through differential proliferation, migration and cell polarity (Matsui and Bessho, 2012). The genetic programs that establish left-right asymmetry in vertebrates are largely conserved, but the timing of laterality signals and structure of the organs that generate asymmetry vary between vertebrate classes (Beyer et al., 2012). In many vertebrates, motile cilia in a transient embryonic structure – the ventral node in mouse, Kupffer's vesicle in zebrafish or the gastrocoel roof plate in *Xenopus* (Essner et al., 2005; Kramer-Zucker et al., 2005; Nonaka et al., 2002; Schweickert et al., 2007) – generate a net leftward fluid flow that leads to the commitment of each side to a left or right identity (Buceta et al., 2005; Cartwright et al., 2004; Nonaka et al., 2002; Nonaka et al., 2005; Okada et al., 1999). Asymmetric activity of ion channels at cleavage stages specifies lateral fates in some species (Aw et al., 2008; Fukumoto et al., 2005; Kawakami et al., 2005; Levin et al., 2002); this early activity may specify but does not determine laterality except in chick. Mutations that affect cilia polarity (Kishimoto et al., 2008; May-Simera et al., 2010; Serluca et al., 2009; Wang et al., 2011), outgrowth (Bisgrove et al., 2012, 2005; Ravanelli and Klingensmith, 2011) or movement all disrupt laterality determination (Essner et al., 2005; Olbrich et al., 2002).

In all vertebrates examined, the asymmetric activation of second messengers on the left side of the laterality organ triggers expression in the left lateral plate mesoderm of a Nodal-related gene such as *southpaw* (spaw) in zebrafish (Long et al., 2003; Levin et al., 1995; Lowe et al., 1996). Nodal expression expands rostrally on the left side of the embryo (Wang and Yost, 2008) through a self-enhancement and lateral inhibition (SELI) mechanism (Nakamura et al., 2006). Left-sided Nodal activity leads to expression of the transcription factor *pitx2* on the left side of the viscera, brain and heart (Campione et al., 1999; Essner et al., 2000; Saijoh et al., 2000; Shiratori et al., 2001; Yoshioka et al., 1998) and activates *lefty1* and *lefty2* on the left side of the brain and heart, respectively (Bisgrove et al., 1999; Long et al., 2003; Meno et al., 1997; Meno et al., 1996). In the zebrafish embryo, disruption of cilia motility in Kupffer's vesicle (KV) alters *southpaw* expression (Kishimoto et al., 2008; May-Simera et al., 2010; Serluca et al., 2009; Wang et al., 2011; Bisgrove et al., 2012, 2005; Ravanelli and Klingensmith, 2011). If the wave of *spaw* expression first reaches its rostral-most extent on one side, downstream laterality genes may be expressed on that side only, resolving the asymmetry but randomzing its direction (Wang and Yost, 2008). The misdirection of the global vector of asymmetry leads to the concordant reversal of the internal organs and brain asymmetry (Chen et al., 2001; Bisgrove et al., 2003). However, embryos that express laterality genes on both sides may fail to develop asymmetry, leading to heterotaxy, in which organs have two left or right sides, and fail to migrate correctly. The expression of midline antagonists to Nodal signaling is essential to prevent the contralateral expansion of *spaw*. Disruption of the Nodal inhibitors *charon* in the peri-KV region (Lopes et al., 2010), *lefty1* in notochord, and *lefty2* in heart (Lenhart et al., 2011; Saijoh et al., 2000), or of BMP4 near KV (Chocron et al., 2007) all lead to discordant directions of asymmetry between the organs (Chen et al., 2001; Chin et al., 2000). In the final phase of the establishment of asymmetry, individual organs interpret the molecular laterality cues by executing organ-specific asymmetric behaviors. Asymmetric gene expression leads to asymmetric migration, growth or tension on the organ precursors, resulting in a leftward migration (jog) of the atrial end of the heart (Glickman and Yelon, 2002; Smith et al., 2008), a leftward bend of the gut (Horne-Badovinac et al., 2003; Kurpios et al., 2008), and asymmetric growth of the epithalamus and parapineal organ in the brain (Gamse et al., 2005). At this stage, the concordance of asymmetry depends on the interpretation of laterality signals by each individual organ.

In this paper we explore the early expression and function of *hspb7* and *hspb12* during the establishment of laterality and the migration of the heart fields. Both genes are expressed in the yolk syncytial layer (YSL) and in the bilateral heart fields, and *hspb7* is transiently expressed in Kupffer's vesicle. We find that *hspb7* and *hspb12* are required for the establishment of left-right asymmetry of the heart, as well as of the brain and the gut, although they have different effects on the concordance of asymmetry between these organs. We demonstrate that reduced *hspb7* inhibits cilia motility in KV by converting motile 9+2 KV cilia to 9+0 cilia.

Methods

Fish lines

Morpholino oligonucleotide (MO) injections were performed in the transgenic *Danio rerio* line *Tg*(*cmlc2:GFP*) (Burns et al., 2005), which expresses green fluorescent protein in heart muscle under the *myl7* (*cmlc2*) promoter. A small number of morpholino experiments were performed in Tg(cmlc2:GFP) crossed to a pet store line (Flanagan-Steet et al., 2005). In situ hybridizations (ISH) for *hspb7*, *hspb12*, *Nkx2.5* and *myl7* were performed in the AB* line on uninjected embryos. ISH for *spaw*, *lefty1*, *lefty2*, *pitx2*, *foxa3* and *myl7* was performed on MO injected *Tg*(*cmlc2:GFP*) embryos. Injected embryos were raised at 28.5 °C in E2 medium (15 mM NaCl, 0.5 mM KCl, 1.0 mM $CaCl_2$, 1.0 mM $MgSO_4$, 0.15 mM KH_2PO_4, and 0.7 mM $NaHCO_3$) supplemented with 10 μM gentamycin (Westerfield et al., 2009), and staged by somite count or by equivalent hours post-fertilization (hpf) (Kimmel et al., 1995).

Morpholino oligonucleotide injections

hspb7, *hspb12*, and control antisense morpholino oligonucleotides (MOs) were obtained from Gene Tools (Philomath, OR). Hspb7MO1 targeted the exon1/intron1 boundary TGCATATAGCTTTCCACTCACTTGG. Hspb7MO2 spanned the intron1/exon2 boundary, GCCTGTTCTGTCTGATGAAAAACAT. Hspb12MO1 targeted the exon1/intron1 boundary, CTAGCCACATAAAATCTCGACCTTGG, and hspb12MO2 targeted the exon2/intron2 boundary, GCTC CTCGCTTACTCTTTATGTGGT. Control embryos were injected with standard negative control human β-globin MO (Gene Tools). Morpholinos were diluted to 0.5 mM in nuclease-free water containing 0.1% phenol red and injected into embryos in a volume of approximately 1 nL. Injections were delivered with MPPI-2 air-powered injectors (Applied Scientific Instrumentation, Eugene, OR). Yolk injections were performed between 3–4.3 hpf. Fluorescein-conjugated

control MO (0.125 mM) was included in MO mixtures for yolk injection. Successfully yolk-injected embryos retained the phenol red color for 5 min post-injection; an immediate change of the injected fluid to yellow predicted the failure of the MO to be distributed through the yolk.

Quantitative PCR

Quantitative PCR for *hspb7* and *hspb12* was performed as previously described (Elicker and Hutson, 2007).

In situ hybridization

Following fixation in 4% formaldehyde at the appropriate developmental stage, in situ hybridization (ISH) was performed as previously described (Thisse and Thisse, 2008). *spaw*, *lefty1*, *lefty2*, and *pitx2c* probes were the kind gifts of Joe Yost; *nkx2.5*, and *myl7* (*cmlc2*) were the generous gifts of Deborah Yelon; *foxa3* probe was obtained from ATCC (Manassas, VA, USA). *hspb12* probe was previously described (Marvin et al., 2008). A 1057 bp *hspb7* probe was amplified by PCR from IMAGE clone 7233563, and transcribed from a T7 promoter incorporated into the 3′ primer. Constructs containing the probes were linearized and transcribed in the antisense direction with the appropriate prokaryotic RNA polymerase (T7: Promega; SP6; Roche Applied Science) in the presence of DIG labeling mix (Roche Applied Science).

Cilia motility and fluid flow in Kupffer's vesicle

To analyze motile cilia or fluid flow in Kupffer's vesicle (KV), live embryos were dechorionated and mounted in 1% low melting point agarose. Beating cilia were imaged between the 8–10 somite stages and fluorescent beads (Polysciences, Inc.) injected into the KV lumen as described (Amack and Yost, 2004; Essner et al., 2005) were imaged between the 6–10 somite stages to visualize fluid flow. Movies were captured using a Zeiss Axiocam high-speed monochromatic camera on a Zeiss AxioImager MI microscope with a 63× water-dipping objective. These movies were analyzed and edited using AxioVision (Zeiss), ImageJ (NIH) and Quicktime (Apple) software.

Transmission electron microscopy

Embryos were fixed at 10 somites in 2.5% glutaraldehyde and 2% formaldehyde in 0.1 M sodium cacodylate solution at 4 °C, overnight and washed in 0.1 M sodium cacodylate. Secondary fix was 3 h in 1% OsO_4. Embryos were washed in deionized water, dehydrated through an ethanol series, followed by a propylene oxide/resin series. Resin-embedded embryos were cured at 60 °C overnight. Thin sections through KV were stained for 7 min in 2% uranyl acetate in a 50:50 mix of ethanol and methanol, followed by 2% lead citrate for 2 min (Bozzola and Russell, 1992). Sections were mounted on copper grids and imaged on a Philips CM 10 transmission electron microscope.

Rescue constructs for hspb7 and hspb12

Three Danio rerio *hspb7* expression constructs were created from an EST (IMAGE clone 7623563; GenBank Accession no. BC083373). Tol2-CMV-hspb7: the coding region of *hspb7* was amplified by PCR with nested primers containing a consensus Kozak sequence and attB1 and attB2 sites and cloned into a Tol2 plasmid using the Gateway system (Invitrogen). CS2+hspb7: the coding region of hspb7 was amplified using primers engineered to create a BamH1 site upstream of the ATG and an Xba1 site at the stop codon, and cloned into corresponding sites on CS2+. CS2+hspb7EST: the hspb7 EST was cut with Not1 and blunted, then EcoR1. The 1150 bp fragment containing the entire cDNA was cloned into CS2+ cut with EcoR1 and Stu1. CS2+Hu-hspb7-myc: Frt-TO-myc-Huhspb7 (Vos et al., 2009; kind gift from Dr. Harm Kampigna) was cut with Dra1 and ligated to CS2+ cut with Stu1. CS2+hspb12: the coding region of *hspb12* was amplified from an EST (Genbank Accession no. CK689325) with primers conferring a BamH1 and Xba1 site at the 5′ and 3′ ends respectively, and ligated to CS2+ cut with the same enzymes. In vitro transcripts were generated using mMessage Machine (Ambion) from linearized plasmids using SP6, and purified with MegaClear (Ambion).

Results

Expression of hspb7 and hspb12 in the early zebrafish embryo

Our previous survey of the expression of small heat shock proteins demonstrated that three zebrafish *shsps* are expressed in heart at 24–48 h post-fertilization (hpf) (Marvin et al., 2008). Here, we extend the description of *hspb7* and *hspb12* expression patterns to earlier stages. Transcripts for *hspb7* and *hspb12* were not detected at 2 or 4 hpf by in situ hybridization (ISH) or quantitative RT-PCR. *hspb7* and *hspb12* expression was first detected by ISH at 5.7 hpf in the yolk syncytial layer (YSL; Fig. 1A and E). Transient *hspb7* expression was observed in the developing KV (arrows in Fig. 1B and C) at the one-somite stage, but this KV expression was undetectable by the 4-somite stage (Fig. 1D). In contrast, *hspb12* was not observed in KV (Fig. 1F and G). Both *hspb7* and *hspb12* were expressed in the YSL from 5.7 hpf through the 4-somite stage (Fig. 1D and H), but disappeared by 10 somites. *hspb7* expression began in the bilateral heart fields at the 12 somite stage (Fig. 1I) and remained concentrated in the precardiac mesoderm during its migration toward the midline (Fig. 1J). *hspb12* expression commenced in the bilateral cardiac precursors several hours later, at the 18 somite stage (Fig. 1K); at this stage the *hspb7* and *hspb12* expression patterns resembled that of *nkx-2.5*, which is localized to the ventricular precursors (Fig. 1L). After fusion of the bilateral cardiac fields at 21–22 somites, expression of both *hspb7* (Fig. 1M) and *hspb12* (Fig. 1N) continued. The *hspb12* domain appeared larger on the left in some embryos (Fig. 1N); this asymmetry was transient. Compared to the expression domain of *myl7* at 22 somites (Fig. 1O), *hspb7* and *hspb12* were localized to a subset of the heart field. Their expression was maintained in ventricle until at least 48 hpf, and intensified in the atrioventricular canal and outflow tract between 24 and 48 hpf (Marvin et al., 2008).

Global depletion of hspb7 altered heart development

To investigate the roles of *hspb7* during embryonic development, we designed a splice-blocking morpholino (hspb7MO1) against the exon 1–intron 1 boundary of *hspb7* to disrupt processing and translation of *hspb7* transcripts. At 26 hpf, the direction of the heart jog was randomized in embryos injected with 0.5 pmole of hspb7MO1 (Fig. 2A), while the hearts of control MO injected embryos consistently jogged to the left (Fig. 2A and B). In situ hybridization for *myl7* demonstrated that the heart tubes that jogged to the right in hspb7MO1-injected embryos were abnormally shaped. The atrial ends were more rounded, and the heart was shorter and wider compared to control MO injected embryos (Fig. 2C). At 24 hpf, control MO-injected embryos had a normal axis and straight trunk (Fig. 2D), but *hspb7* morphants developed a downwardly curved body axis (Fig. 2E), a phenotype characteristic of cilia defects (Kishimoto et al., 2008; Serluca et al., 2009). Despite the axis curvature, the length of *hspb7* morphants ($n=6$) from the otic vesicle to the tip of the tail was 101 (±2%) of control MO embryos ($n=5$), suggesting that convergent extension defects did not contribute to the phenotype. Injection of 0.5 pmole of

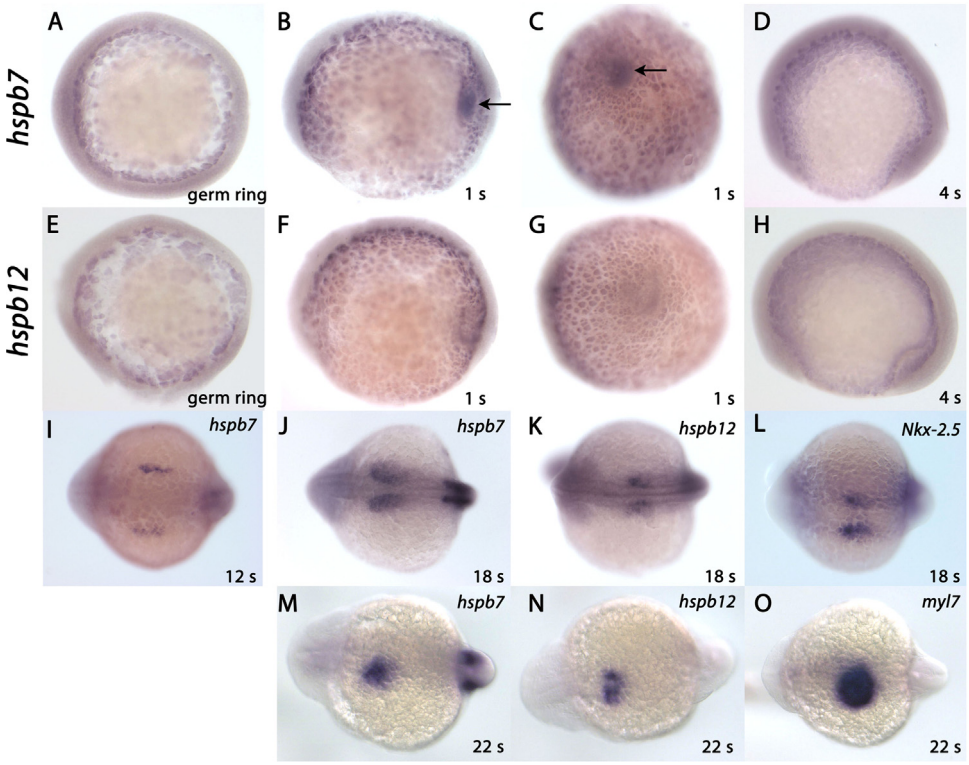

Fig. 1. Expression patterns of *hspb7* and *hspb12* during the first 22 h of development. (A) *hspb7* was first detected by in situ hybridization at 5.7 hpf in the yolk syncitial layer (YSL) (B) *hspb7* expression continued in the YSL and was transiently expressed in the forming Kupffer's vesicle (KV) at the tailbud-1 somite stage. (C) Posterior view of *hspb7* expression in KV (arrow) at tailbud stage (dorsal to the left). (D) *hspb7* disappeared from KV (arrow) by the four somite stage but remained in the YSL. (E) *hspb12* was similarly expressed in the YSL at 5.7 hpf. (F) *hspb12* was expressed in the YSL at 1-somite stage, but was not detected within KV. (G) Posterior view showing that *hspb12* hybridization was not visible in KV. The surface of the YSL is depressed beneath the tailbud. This causes an edge-on view of the YSL surface, but the apparent staining was not visible at other angles. (H) *hspb12* was absent from KV in four somite stage embryos, but YSL expression continued until approximately the 10 somite stage. (I) *hspb7* was expressed in the bilateral heart fields beginning at the 12 somite stage. (J) *hspb7* in the heart field and somites at the 18 somite stage. (K) *hspb12* expression began in the bilateral cardiac precursors at the 18 somite stage. (L) *Nkx-2.5* is expressed in ventricular precursors and corresponds to the expression sites of *hspb7* and *hspb12* at 18 somites. (M) *hspb7* and (N) *hspb12* were expressed in the fused heart fields as the leftward jog of the primitive heart tube begins at 21 somites. (O) Expression of *myl7* (*cmlc2*) at 21–22 somites overlapped *hspb7* and *hspb12* hybridization.

hspb7MO1 reduced *hspb7* mRNA to 25–61% of control levels at 24 and 26 hpf, respectively (Supplementary Fig. 1).

To test the specificity of hspb7MO1 phenotypes, we designed a second MO (hspb7MO2) to target the intron 1–exon 2 splice acceptor site. At a dose of 0.25 pmole, hspb7MO2 also disrupted asymmetry (Fig. 2A) and induced downward-curling tails at 24 hpf. Higher doses of hspb7MO2 were generally lethal; the surviving embryos' hearts failed to jog and remained at the midline (data not shown). A third morpholino, which blocks *hspb7* translation (Musso et al., in press) caused similar degrees of midline and right heart jogs (data not shown). Thus, three morpholinos against *hspb7* produced similar laterality phenotypes.

Greater degrees of gene knockdown can be obtained by combining two MOs directed at the same gene (Draper et al., 2001). We therefore combined a reduced dose of hspb7MO1 with hspb7MO2 (0.25 pmol each) and injected this combination into embryos at the 1–4 cell stage. The combination of the two MOs reduced *hspb7* transcripts to 12% of normal levels at 24 hpf (Supplementary Fig. 1). This stronger knockdown led to a further reduction in the number of embryos with normal leftward-jogging hearts than was induced by either of the *hspb7* MOs alone (Fig. 2F and G). The midline hearts resulting from the combined *hspb7* MOs were short and wide (Fig. 2H). Even in embryos with leftward-jogging hearts, there appeared to be a defect in heart migration; the leading edge of the cardiac primordia just reached the posterior extent of the eye, while the leading edge of the heart field in control embryos lay at the anterior–posterior midpoint of the eye (Fig. 2I). Moreover, the combined *hspb7* MOs caused cardia bifida in some embryos, in which the bilateral heart fields fail to migrate to the midline and fuse (Fig. 2J). Cardia bifida was never observed in control MO or single *hspb7* MO-injected embryos. These data suggest that *hspb7* supports cardiac mesoderm migration, in addition to its function in establishing left–right asymmetry of the heart. However, asymmetry is more sensitive to the dose of *hspb7* than is heart precursor migration.

hspb7 depletion in the yolk disrupted cardiac movements

The fusion of cardiac primordia depends upon the integrity of the YSL extracellular matrix; mutations and morpholinos that disrupt either the YSL or definitive endoderm cause cardia bifida (Alexander et al., 1999; Arrington and Yost, 2009; Dickmeis et al., 2001; Kikuchi et al., 2001; Sakaguchi et al., 2006). Both the YSL and the precardiac mesoderm express *hspb7*, so depletion of *hspb7* in either tissue could be responsible for the cardiac migration defect. To distinguish between these possibilities, we took advantage of the finding that cytoplasmic bridges between the yolk and most embryonic tissues close by the 256-cell stage (Kimmel and Law, 1985). MO injected to the yolk prior to sphere stage (4 hpf) is taken up by the yolk syncyctial layer, and at a lower efficiency by the dorsal forerunner cells (DFC) that give rise to KV (Amack and Yost, 2004; Arrington and Yost, 2009; Essner et al., 2005). Therefore injecting MO into the yolk cell after the 256-cell stage (~2.5 hpf) restricts the effect of the MO to the YSL and KV. To identify embryos in which yolk-targeted MO was successfully

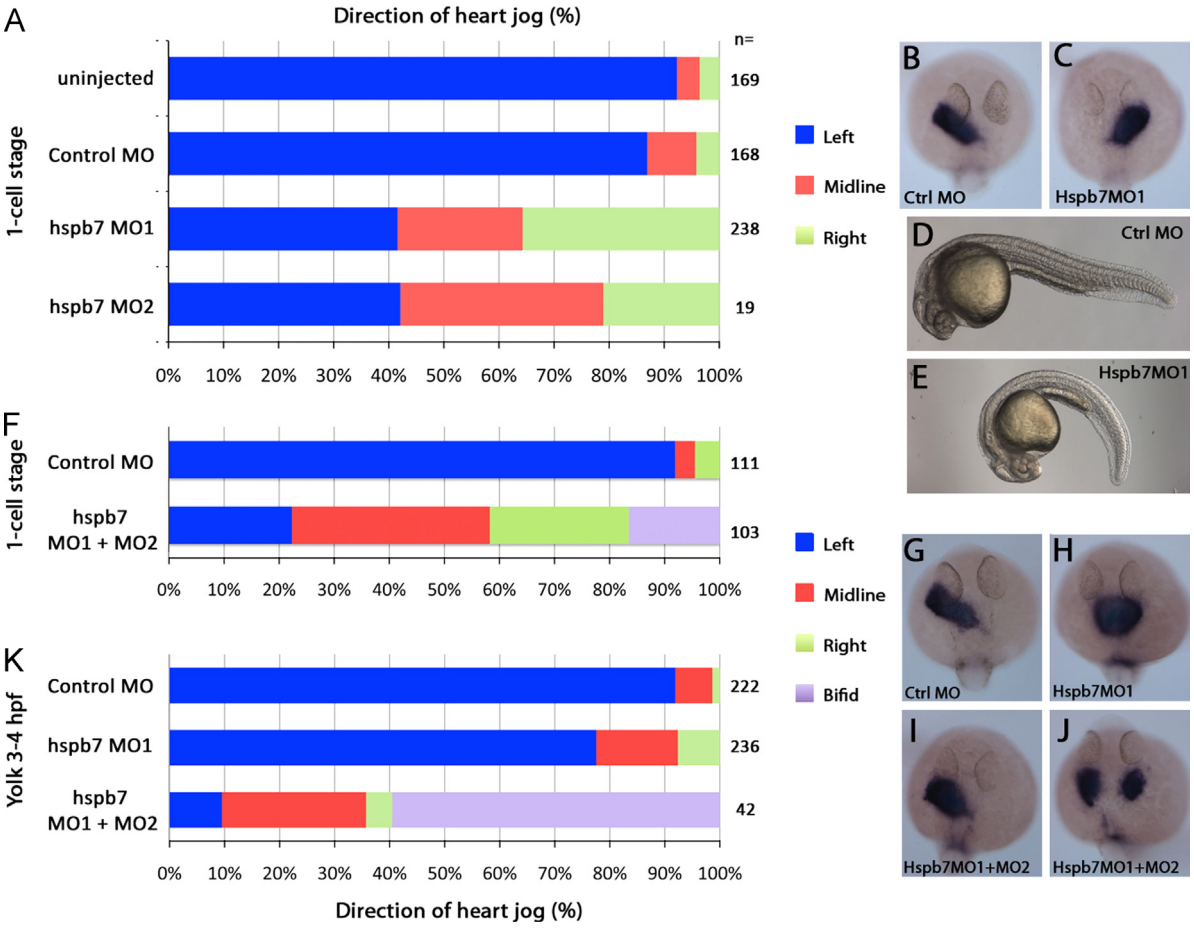

Fig. 2. Heart jog direction was randomized by *hspb7* knockdown. (A) Two splice-blocking morpholinos that target *hspb7* both significantly increased right and midline heart jogs at the expense of leftward heart jogs (χ^2 test, $p < 0.001$). (B, C) In situ hybridization of *myl7* (*cmlc2*) in embryos injected with hspb7MO1. (B) Left jog and (C) right jog. (D) Live embryo at 26 hpf, injected with control MO. (E) Live embryo at 26 hpf, injected with hspb7MO1, showing characteristic downward curl of the body. (F) The combination of hspb7MO1 (0.25 pmole) and hspb7MO2 (0.17 pmole) prevented heart field fusion when targeted to the whole embryo at 1–4 cell stages. (G–I) In situ hybridization for *myl7* (*cmlc2*). (G) Embryo injected with control MO at 1 cell stage had normal leftward heart jogs; the anterior boundary of the heart is midway across the eye at 26 hpf. (H) Midline heart in embryo injected with hspb7MO1+MO2 at 1 cell stage, showing slowed anterior migration, with the anterior boundary of the heart at the posterior end of the eye. (I) hspb7MO1+MO2 injected embryo, with normal leftward jog but delayed anterior migration and wide heart. (J) hspb7MO1+MO2 injected embryo, with cardia bifida. (K) Yolk injection between 3 and 4 hpf of control MO produced a small number of midline hearts; hspb7MO1 (0.5 pmole) induced midline hearts; hspb7MO1 (0.25 pmole) and hspb7MO2 (0.25 pmole) induced cardia bifida and midline hearts.

distributed throughout the YSL, we included 0.1 pmol of fluorescein-conjugated control MO as a tracer. Over 60% of injected embryos showed fluorescent MO distributed throughout the YSL exclusively at 50% epiboly; the remainder of the embryos had the MO trapped in yolk granules. Distribution of the MO to the embryo itself was never observed, confirming previous studies of yolk injection (Amack and Yost, 2004; Arrington and Yost, 2009). Injection of hspb7MO1 (0.5 pmol) into the yolk cell at 3–4 hpf increased the frequency of abnormal heart jogs compared to control MO (Fig. 2K). A strong yolk-targeted knockdown of *hspb7* by the combined hspb7MO1 and hspb7MO2 (0.25 pmole each) induced cardia bifida, midline hearts, and altered anterior migration. Cardia bifida precludes analysis of laterality; the direction of jogging in bifid hearts cannot be determined. The distribution of heart phenotypes differs signficantly ($\chi^2 = 58.3$, $p < 0.001$) between hspb7MO1+MO2 injected to the yolk compared to injection of this MO pair at the 1–4 cell stage (Fig. 2F and K), suggesting that restricting the injection to the yolk causes a more severe migration defect by concentrating the morpholino there.

hspb12 is necessary for normal cardiac laterality

Depletion of *hspb12* also caused cardiac left–right asymmetry defects (Fig. 3A). A morpholino that targets the exon 1–intron 1 boundary (hspb12MO1) reduced expression levels of the endogenous transcript to 12–21% of control levels at 26 hpf (Supplementary Fig. 1). hspb12MO1 (0.5 pmol) caused an increase in midline and right-sided hearts, compared to control MO (Fig. 3A). In embryos injected with a second MO that targets the *hspb12* exon 2–intron 2 boundary (hspb12MO2), the frequency of midline and right hearts also differed significantly from control MO (Fig. 3A). A dose of 0.125 pmol hspb12MO2 was optimal; higher doses had toxic effects. A combination of the two *hspb12* MOs resulted in incomplete gastrulation even at low combined doses, so the effects of a stronger *hspb12* knockdown could not be assessed.

hspb12 and heart migration

YSL-targeted injections of hspb12MO1 increased the proportion of midline hearts compared to control MO (Fig. 3B). There was no significant difference in the distribution of heart laterality for hspb12MO1 injections into the yolk versus the whole embryo (Fig. 3A and B), although the number of right heart jogs appeared to be lower for the yolk injections. hspb12MO1 did not induce cardia bifida in the Tg(cmlc:GFP) AB background. However, occasional cardia bifida was observed in yolk injections in a Tg(cmlc:GFP) in

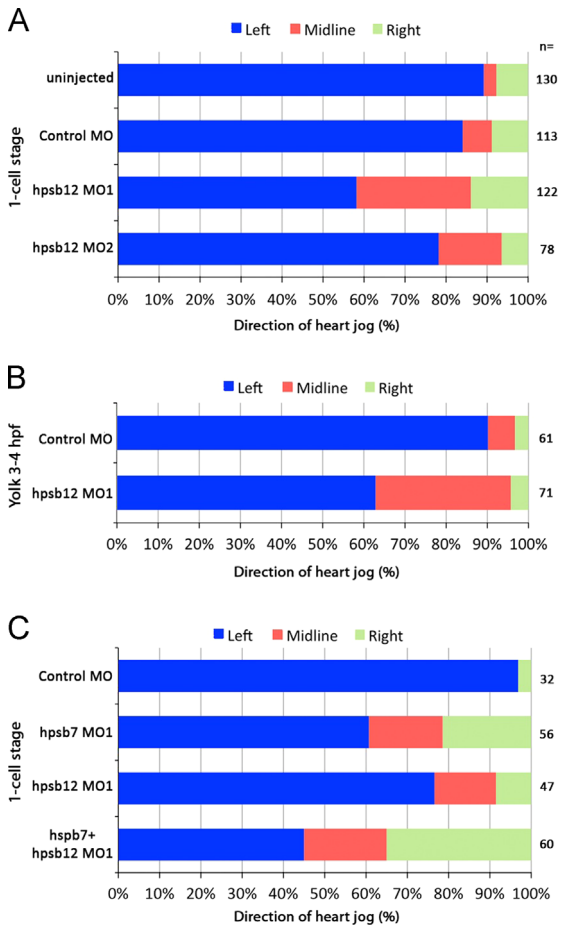

Fig. 3. Heart jog direction was randomized by *hspb12* knockdown (A) Two morpholinos that target *hspb12* significantly increased right and midline heart jogs at the expense of leftward jogs compared to control MO (χ^2 test; $p<0.001$ for hspb12MO1 and $p<0.05$ for hspb12MO2). (B) Yolk injections of hspb12MO1 increased midline hearts but not rightward jogs. Combinations of both hspb12 MOs were lethal. (C) Combined hspb7MO1 and hspb12MO1 (0.25 pmol individually or in combination) injected at the 1-cell stage increased midline hearts and rightward jogs significantly compared to control (χ^2 test; all $p<0.001$). Combined hspb7MO1 + hspb12MO1 (0.25 pmol each) gave significantly more abnormal jogs than 0.25 pmol hspb7MO1 alone (χ^2 test; $p<0.05$).

another wild type background, which is more sensitive to *hspb12* knockdown (Supplementary Fig. 2).

Functional overlap between hpsb7 and hspb12

Of all the sHsps, *hspb12* is most similar to *hspb7* in the conserved α-crystallin domain. Their expression patterns are similar, although *hspb12* was not detected in KV, suggesting that there could be functional redundancy between the two genes. To investigate this possibility, hspb7MO1 and hspb12MO1 were co-injected into 1-cell embryos. At doses for which each MO individually had a submaximal effect, the combination caused an increase in laterality defects (Fig. 3C). The combination of 0.25 pmol Hspb7MO1 and 0.25 pmol Hspb12MO1 increased the frequency of abnormal laterality so that it did not statistically differ from that caused by 0.5 pmole of Hspb7MO1 alone (Fig. 2A), suggesting that there is a functional overlap between *hspb7* and *hspb12*.

Reduced hspb7 expression affects laterality genes

The first asymmetrically expressed gene in zebrafish is *southpaw* (*spaw*) in the left lateral plate mesoderm. This *nodal*-related gene induces the transcription factor *pitx2* in the left lateral plate and brain, as well as the Nodal inhibitors *lefty1* and *lefty2* on the left side of the brain and heart, respectively (Long et al., 2003). Embryos injected with control MO expressed *spaw* in the left lateral plate mesoderm (Fig. 4A and B). However, hspb7MO1 induced primarily bilateral or left sided *spaw* expression at 14–18 somite stages (Fig. 4A and C); few embryos had right-sided expresssion (Fig. 4A).

There are two mechanisms that can result in bilateral expression of *spaw*. When KV cilia function is disrupted or signals from KV fail to transmit to the lateral plate, *spaw* is often expressed bilaterally (Bisgrove et al., 2003, 2005; Francescatto et al., 2010; Hashimoto et al., 2004; Ravanelli and Klingensmith, 2011; Schottenfeld et al., 2007). A second mechanism would be the failure of the midline barrier to block induction of ectopic *spaw* in the right lateral plate by the normal expression of *spaw* on the left. This midline barrier consists in part of KV-independent expression of *lefty1* in notochord (Bisgrove et al., 1999; Meno et al., 1998). Embryos injected with either control MO or hspb7MO1 showed normal expression of *lefty1* in notochord and around KV (Fig. 4B and C), indicating that the midline barrier remained intact.

Many *hspb7* morphant embryos expressed *spaw* bilaterally, but the anterior expansion of *spaw* expression was not equal on the two sides (Fig. 4D and E), such that either the left or the right lateral plate domain was leading. In embryos that expressed *spaw* bilaterally, the lagging domain was typically greater than 75% of the length of the leading side. Of the embryos that expressed *spaw* bilaterally 16.4% had the left leading, 25.4% were equal, 10.4% had the right domain leading. Such unequal bilateral domains have previously been reported in *pkd2* mutants and *casanova*, *lefty1*, and *charon* morphants (Schottenfeld et al., 2007; Wang and Yost, 2008).

Because *hspb7* knockdown caused bilateral *spaw* expression, we would expect a disruption of lateralized gene expression downstream of *spaw*. *pitx2* is a target of lateral plate *nodal* signaling and, consistent with this prediction, the expression of *pitx2* was randomized in hspb7MO1-injected embryos, with equal numbers expressing *pitx2* on the left or right, and a small fraction showing bilateral expression (Fig. 4F). The expression of *lefty2* in the heart field and *lefty1* in the diencephalon also depend upon lateral plate *spaw* expression (Long et al., 2003). A much smaller fraction of embryos injected with hspb7MO1 had bilateral expression of *lefty2* (Fig. 4G) compared to the number of embryos expressing *spaw* bilaterally; *lefty2* was primarily expressed on only the left or right side (Fig. 4H and I). Similarly, expression of *lefty1* in the brain was randomized at approximately the same rate as *lefty2* in the heart field in hspb7MO1 morphant embryos (Fig. 4J), and there was far less bilateral expression than for *spaw*. This frequency was consistent with the heart jog data (Fig. 2A), suggesting that the bilateral expression of *spaw* resolves to unilateral *lefty1* and *lefty2* expression, and results in heart jogs with randomized direction, instead of failure to jog (Fig. 2A).

Reduced hspb12 affects laterality genes

Embryos injected with hspb12MO1 showed an increase in bilateral or right-sided expression of *spaw* at the 14–18 somite stage (Fig. 5A). The degree of this response was dependent on genetic background. Tg(cmlc:GFP) in an AB background (Burns et al., 2005) had a small but statistically significant increase in bilateral expression of *spaw* in response to *hspb12* knockdown (data not shown). However, fish from this line outbred to another wild-type strain (Flanagan-Steet et al., 2005) had a more robust response (Fig. 5A). Embryos injected with hspb12MO1 expressed *lefty1* normally in the notochord, suggesting that the midline barrier remained intact in these embryos (Fig. 5B and C).

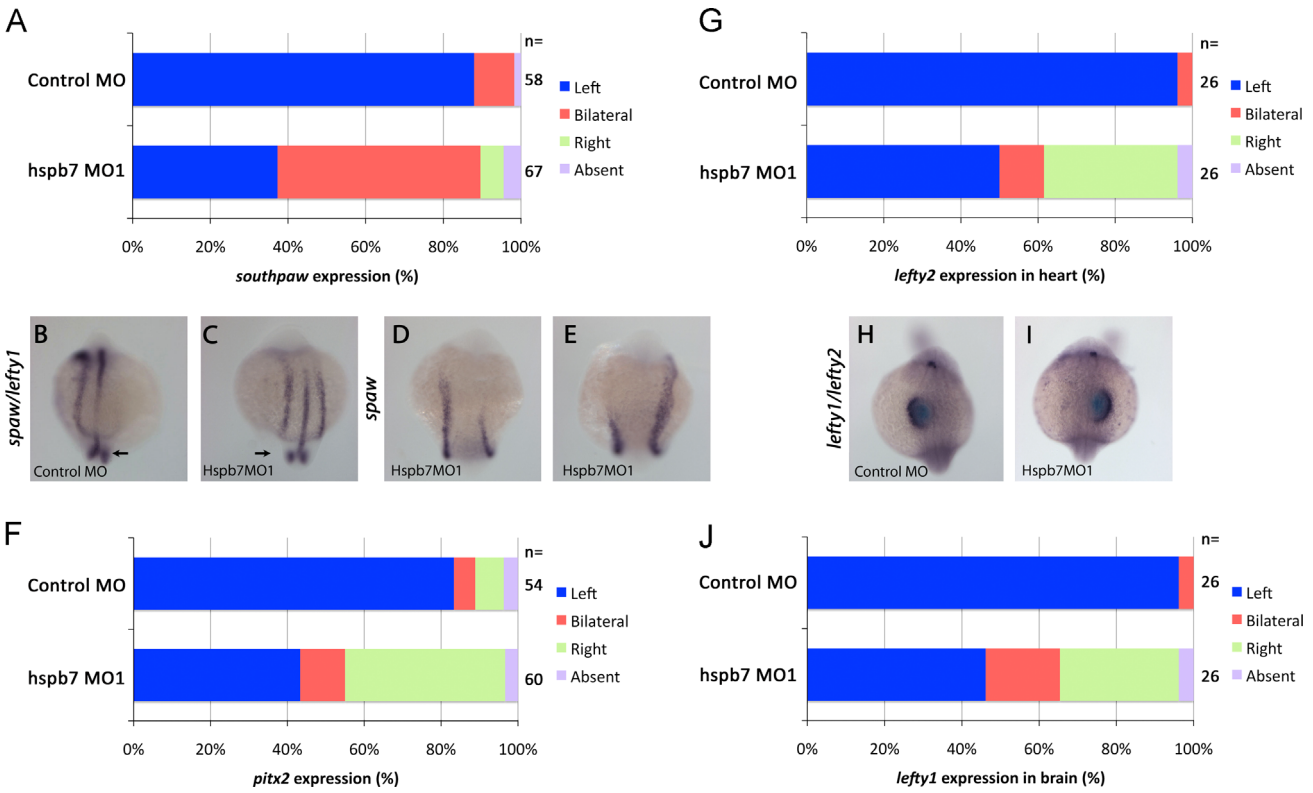

Fig. 4. *hspb7* was necessary for the expression of laterality genes in the left lateral plate mesoderm (LPM). (A) Embryos injected with 0.5 pmol control MO had primarily left-sided expression of *spaw* in the lateral plate mesoderm. In contrast, hspb7MO1 induced bilateral spaw expression (χ^2 test; $p < 0.001$). (B–E) 14–18 somite stage embryos. (B) Embryos injected with control MO had normal *spaw* and *lefty1* expression in left LPM and notochord, respectively. In the tail, bilateral peri-KV *spaw* domains were present (arrow). (C) hspb7MO1-injected embryos expressed *spaw* bilaterally. *lefty1* in the notochord and peri-KV expression of *spaw* were not disturbed. (D, E) hspb7MO1-injected embryo with bilateral spaw with (D) left side leading leading and (E) right side leading. (F) hspb7MO1 randomized *pitx2* expression (χ^2 test; $p < 0.001$), with largely left or right sided expression and a small fraction of bilateral expression. (G) *lefty2* expression in the left heart field was randomized or made bilateral by hspb7MO1 injection (χ^2 test; $p < 0.001$). (H) embryos injected with control MO express *lefty1* and *lefty2* on the left side of the heart and brain at 22–24 somite stages. (I) hspb7MO1 injected embryos expressing *lefty1* and *lefty2* on the right. (J) *lefty1* expression in brain was randomized by hspb7MO1 injection (χ^2 test; $p < 0.001$).

Despite the slight effect on *spaw* expression in the Tg(cmlc:GFP) line with an AB background, knockdown of *hspb12* significantly altered the distribution of the downstream laterality genes *pitx2*, *lefty1* and *lefty2* in this background. Hspb12MO1 (Fig. 5D) induced bilateral, right or absent *pitx2* expression in approximately 38% of the embryos. In many embryos *pitx2* expression in the lateral plate mesoderm was visible but reduced in intensity compared to either control MO embryos or hspb7MO1 injected embryos (data not shown). Injection of hspb12MO1 also perturbed expression of *lefty2* (Fig. 5E) and *lefty1* (Fig. 5I); however, the pattern of changes in gene expression differed notably from those of *hspb7* morphants (Fig. 4G and J). The majority of embryos expressed *lefty1* and *lefty2* on the left (Fig. 5F), but these genes were frequently absent (Fig. 5G), and they were never expressed on the right unless they were mirrored on the left (Fig. 5H). In summary, *hspb12* knockdown affected *pitx2*, *lefty1* and *lefty2* in both strains, but the effect of hspb12MO1 on *spaw* varied by strain.

Redundance of hspb7 and hspb12

At doses that individually had little effect on *spaw*, the combined knockdown of *hspb7* and *hspb12* caused an increase in bilateral and right-sided *spaw* (Fig. 5J). This observation is consistent with the increased cardiac laterality defects in combined *hspb7–hspb12* morphants (Fig. 3C). Although reduced *hspb12* alone did not increase bilateral *spaw* (Fig. 5A), it potentiated the effect of a sub-optimal dose of hspb7MO1 (Fig. 5J). The combined *hspb7* and *hspb12* knockdown also increased the frequencies of embryos with right-sided or absent *lefty2* and *lefty1* expression (Fig. 5K and L), compared to knockdown of either gene alone. Suppression of right-sided *lefty1* and *lefty2* was characteristic of *hspb12* but not *hspb7* knockdown.

Concordance of laterality defects with reduced hspb7

The intact midline expression of *lefty1* led us to investigate whether the laterality of brain, heart and gut are globally coordinated in *hspb7* and *hspb12* knockdown embryos. If the midline barrier function were disrupted, organs would be randomly oriented relative to each other (Bisgrove et al., 2000; Chin et al., 2000), and few of the embryos would show agreement between the laterality of any two organs. Discordant asymmetry could also occur if there were a disruption in the interpretation of the Nodal laterality signal by the downstream organs (Hirokawa et al., 2009; Ramsdell, 2005; Raya and Belmonte, 2006).

Expression of *lefty1* and *lefty2* in control embryos was concordant, with both genes localized on the left in 96.2% of the cases (Table 1). In embryos injected with hspb7MO1, expression of *lefty1* in brain and *lefty2* in heart at 22–24 somites were still largely concordant; *lefty1* and *lefty2* were both localized to the left or the right in 77.0% of the morphants (Table 1). The remaining embryos had either bilateral expression of *lefty1* and *lefty2*, indicating an ongoing failure to specify a global vector of asymmetry, or they had discordant expression of *lefty1* and *lefty2*. In these cases one *lefty* gene was expressed normally while the other was abnormal (Table 1).

To investigate concordance between heart and gut turning, we compared the expression of *foxa3* in liver and gut to *myl7*

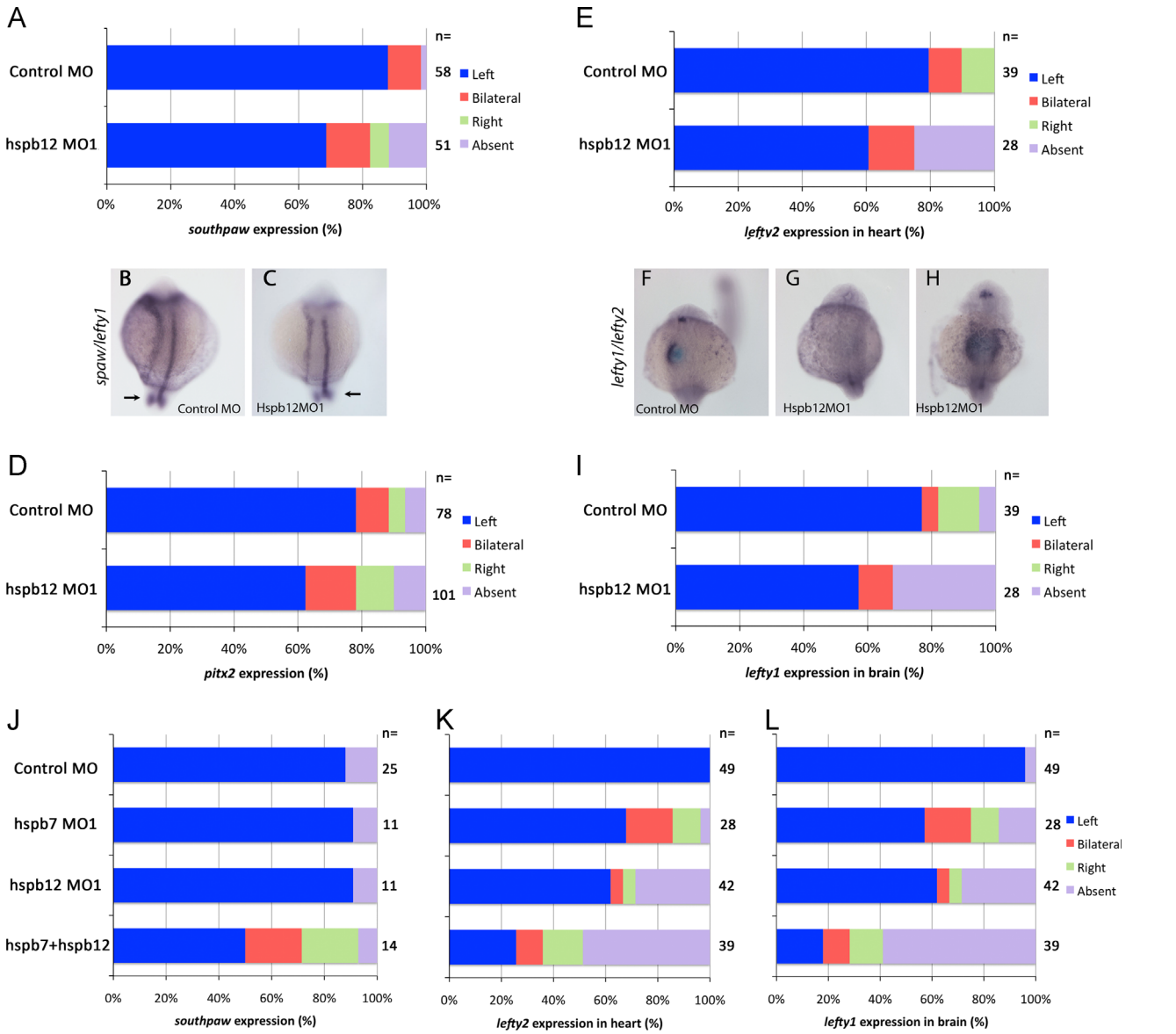

Fig. 5. *hspb12* knockdown randomized *spaw, pitx2*, *lefty2* and *lefty1*. (A) 0.5 pmol hspb12 MO1 increased bilateral *spaw* expression compared to control MO (χ^2 test; $p<0.001$). (B, C) 14–18 somite embryos. (B) Control MO injected embryo with left sided *spaw* and midline *lefty1* expression. (C) hspb12MO1-injected embryo with normal *spaw* and *lefty1* expression. (D) Hspb12MO1 randomized *pitx2* expression (χ^2 test; $p<0.001$). (E) hspb12 MO1 injection did not induce ectopic *lefty2*, but increased the number of embryos lacking *lefty2* expression (χ^2 test; $p<0.001$). (F–H) *lefty1* and *lefty2* in situ hybridization at 22–24 somites. (F) Control MO with normal *lefty1* and *lefty2* in left brain and heart field respectively. (G) In this embryo, Hspb12MO1 suppressed normal *lefty1* and *lefty2*. (H) In another embryo, Hspb12MO1 induced bilateral *lefty1* and *lefty2*. *lefty1* and *lefty2* were never observed exclusively on the right. (I) Hspb12MO1 injection caused bilateral or absent *lefty1* expression in the brain (χ^2 test; $p<0.001$). (J) Injection of 0.25 pmole of hspb7MO1 or hspb12MO1 individually did not affect left-sided spaw expression in the LPM, but injection of both MO together induced bilateral and right-sided *spaw*. (K) A dose of 0.25 pmole of hspb12MO1 or hspb7MO1 individually perturbed expression of *lefty2* in heart, while the combination of 0.25 pmole each of hspb7MO1 and hspb12MO1 induced an even greater degree of abnormal expression. (L) Similarly, 0.25 pmole of hspb7MO1 or hspb12 MO1 induce a similar alteration in the expression of *lefty1* in the brain, while the combination induces further abnormal expression.

expression in heart at 48 hpf. In 95% of control MO-injected embryos, *myl7* expression showed that the atrium was on the left, and that the ventricle had looped to the right, while *foxa3* expression indicated the liver was on the left and the gut had a leftward bend. (Fig. 6A and A′; Table 2). In 82.6% of embryos injected with hspb7MO1, the asymmetry of the gut was concordant with that of heart (Fig. 6B and B′; Table 2). The discordant arrangements (17.4%) were due to hearts that failed to deviate from the midline. We did not observe any duplicated or midline livers or digestive tracts; in embryos with midline hearts, the gut was bent either to the left or the right (Table 2).

hspb7 morphant embryos exhibited a high degree of concordance between both the laterality of the heart and brain, and between the heart and gut. While a fraction of embryos failed to specify a direction of laterality, the expression of *lefty1* and *lefty2*, as well as the direction of heart jogging and gut turning were in agreement, indicating that laterality was not randomly determined for each organ, as would be the case if the midline barrier had been disrupted.

Concordance of laterality defects with reduced hspb12

In hspb12MO1 morphants, only 10.7% of the embryos had discordant brain and heart asymmetry; an equal number had bilaterally symmetric expression of *lefty1* and *lefty2* at the 22–24 somite stage (Table 1). The frequency of discordance and bilateral

lefty1 and *lefty2* expression was similar to that in *hspb7* morphants. However, 25% of *hspb12* morphants lacked both *lefty1* and *lefty2* expression, and there were no embryos with exclusively right-sided expression of the *lefty* genes. While the high frequency of absent expression of *lefty1* and *lefty2* was clearly abnormal, the lack of expression of both genes was still in agreement, indicating that the disruption of laterality determination caused by hspb12MO1 affects both heart and brain in the same manner.

The heart–gut laterality of *hspb12* knockdown embryos was less concordant than heart–brain laterality. Instances of diverse arrangements of laterality were represented (Table 2). Bilateral or absent livers were rare; midline hearts were primarily associated with left or right livers (Table 2). Although the liver and gut both depend on *hspb12* to establish the direction of laterality, the laterality of the visceral organs was less firmly linked to heart direction than for *hspb7* knockdown. However, this increase in discordance was primarily due to the failure of midline hearts to jog or loop, while the visceral organs formed on either the left or right, and may therefore reflect a failure of heart migration rather than an uncoupling of heart and visceral laterality.

Table 1
Brain and heart laterality at 22–24 somites in *hspb7*, *hspb12* and double morphant embryos. *lefty2* is normally expressed in the left heart field and *lefty1* in the left epithalamic precursor at this stage. Concordant expression comprises both *lefty* genes on the same side of the embyro.

lefty1 brain, *lefty2* heart	*n*	*L, L* (%)	*B, B* (%)	*R, R* (%)	*A, A* (%)	Discordant (%)
Control	26	96.2	3.8	0.0	0.0	0.0
hspb7 MO1	26	46.2	11.5	30.8	0.0	11.5
Control	39	76.9	5.1	10.3	0.0	7.7
hspb12 MO1	28	53.6	10.7	0.0	25.0	10.7
Uninjected	49	100.0	0.0	0.0	0.0	0.0
hspb7 MO1+hspb12 MO1	39	51.3	0.0	0.0	33.3	15.4

Concordance in hspb7–hspb12 double knockdowns

Double *hspb7–hspb12* morphants also displayed primarily concordant asymmetry (Table 1) between heart and brain. Discordant double *hspb7–hspb12* knockdown embryos consisted of those with bilateral *lefty2* in the heart and left-sided *lefty1* in the brain. The majority of embryos either expressed *lefty1* and *lefty2* on the left, or failed to express these genes at all. This pattern more closely resembled the effect of hspb12MO1 than hspb7MO1.

Attempts to rescue hspb7 and hspb12 morpholinos

We attempted to rescue the effects of the *hspb7* and *hspb12* morpholinos with in vitro transcripts of *hspb7* and *hspb12* RNAs. Three Danio rerio *hspb7* constructs were made, containing different Kozak sequences: a consensus sequence, a BamH1 site or the endogenous 5′ untranslated region. None of the RNAs from these constructs rescued phenotypes induced by hspb7MO1 when

Table 2
Heart and gut laterality at 48 hpf in *hspb7* and *hspb12* morphant embryos. The atrium jogs to the left and the ventricle undergoes a dextral loop by 48 hpf. The liver develops on the left and strongly expresses *foxa3*; the intestine expresses *foxa3* at a lower intensity. Equal numbers of *hspb7* morphants with midline hearts had *foxa3* liver expression on the left or the right (8.7% each); these comprise the discordant embryos. *hspb12* morphants with discordant phenotypes were also largely embryos with midline hearts and left livers (16.7%) or right livers (9.5%) but also included right sided hearts with left livers (4.8%), right heart without liver (2.4%) and left heart with bilateral liver (2.4%). Discordant control embryos had midline hearts with left or right livers.

Heart jog, liver side	*n*	*L, L* (%)	*M, B* (%)	*R, R* (%)	*A, A* (%)	Discordant (%)
Control MO	20	95.0	0	0	0	5.0
hspb7 MO1	23	52.2	0	30.4	0	17.4
Control MO	33	84.8	0	0	0	15.2
hsbp12 MO1	42	57.1	2.4	2.4	0	38.1

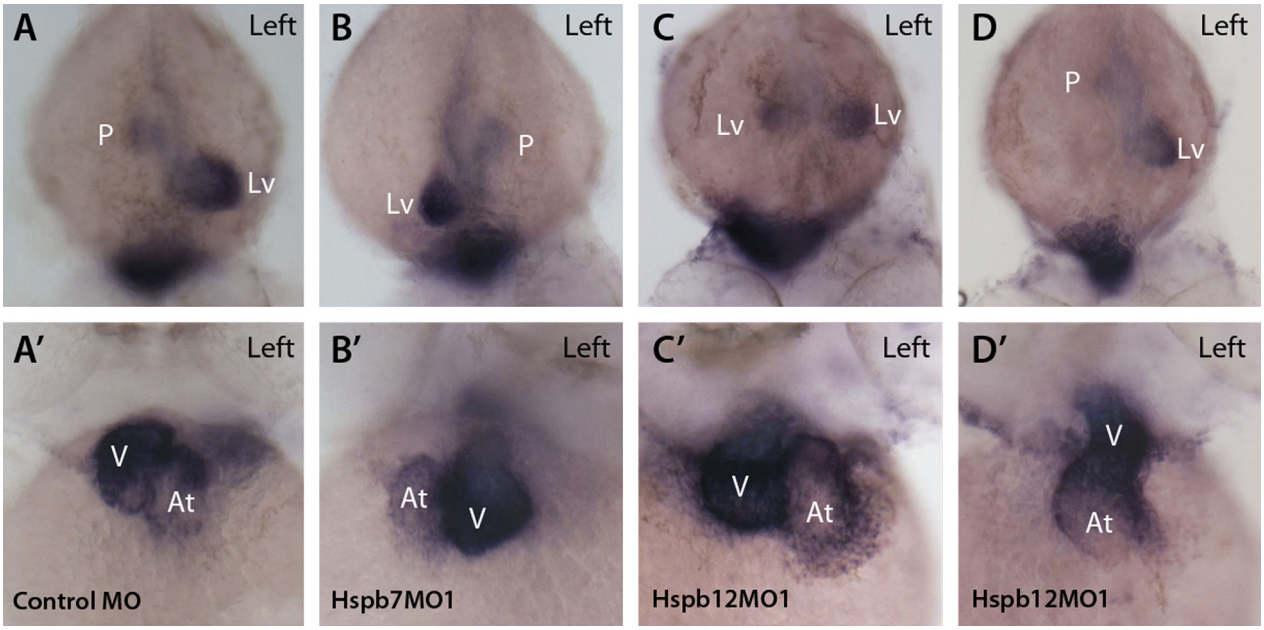

Fig. 6. Concordance of asymmetry between heart and gut in *hspb7* and *hspb12* knockdown embryos. (A–D) Dorsal view, rostral toward bottom, left side as indicated in (A). Expression of *foxa3* is strong in liver (Lv) and weaker in gut and pancreatic bud (P) at 48 hpf. (A′–D′) *myl7* (*cmlc2*) is strongly expressed in ventricle (V) and more weakly in atrium (At) at 48 hpf. Anterior view, left side as indicated in (A). (A, A′) Control MO-injected embryo demonstrated the normal position of atrium to the left of the embryo's midline and of the ventricle on the right (dextral loop). *foxa3* is concentrated in the normal, left-sided liver and weaker in the pancreatic bud in control MO-injected embryo. (B, B′) *hspb7* morphant with right-sided liver and ventricle. (C, C′) hspb12MO1-injected embryo with bilateral liver but normal position of the atrium and ventricle. (D, D′) hspb12MO1-injected embryo with left-sided liver and a heart that failed to jog or loop (midline heart).

injected to the cytoplasm at the 1-cell stage (Supplementary Fig. 3A and B; data not shown). *hspb7* RNA alone had no effect on laterality (Supplementary Fig. 3B). A human *hspb7* construct (Vos et al., 2009) also failed to rescue hspb7MO1-injected embyros. Both the zebrafish and human cDNA constructs produced Hspb7 protein in transfected cultured cells (not shown). qPCR demonstrated the survival of *hspb7* RNA at 50 times the normal level; β-galactosidase enzymatic activity demonstrated the correct targeting of the RNA (data not shown). RNA encoding Danio rerio *hspb12* also failed to rescue defects caused by hspb12MO1 (Supplementary Fig. 3C). Yolk targeting of RNA encoding *hspb7* did not rescue cardia bifida induced by hspb7MO1+MO2 injected to the yolk (Supplementary Fig. 3D). Human Hspb7 is alternatively spliced (Krief et al., 1999), so we searched for alternative transcripts using 5′ and 3′ RACE on mRNA from 12 hpf zebrafish embryos, based on primers within the conserved α-crystallin domain in the second exon of hspb7. These procedures amplified only the known sequence of *hspb7*.

Kupffer's vesicle cilia function

Because defects in the form or function of Kupffer's vesicle can alter *spaw* expression and left–right asymmetry (Amack et al., 2007; Essner et al., 2005), we analyzed KV cilia in hspb7MO1-injected embryos. Many KV cilia in hspb7MO1 injected embryos failed to beat normally. While KV cilia in controls showed rapid vortical beating (Movie 1), cilia in hspb7MO1 injected embryos were often immotile or beat erratically (Movies 2 and 3). Blind scoring of individual cilia revealed that 95% of KV cilia showed normal motility in control MO-injected embryos ($n=183$ from 32 embryos), whereas the number of normal cilia was reduced to 44% in hspb7MO1 fish ($n=109$ cilia from 30 individuals) and 57% in hspb7MO2 embryos ($n=129$ cilia from 26 individuals) (Fig. 7A). To determine whether these cilia motility defects were sufficient to disrupt asymmetric fluid flow in KV, we injected fluorescent beads into the KV lumen. Beads injected into control MO embryos revealed a counterclockwise flow ($n=7/7$; Movie 4 and Fig. 7B) as previously described in wild-type embryos (Essner et al., 2005).

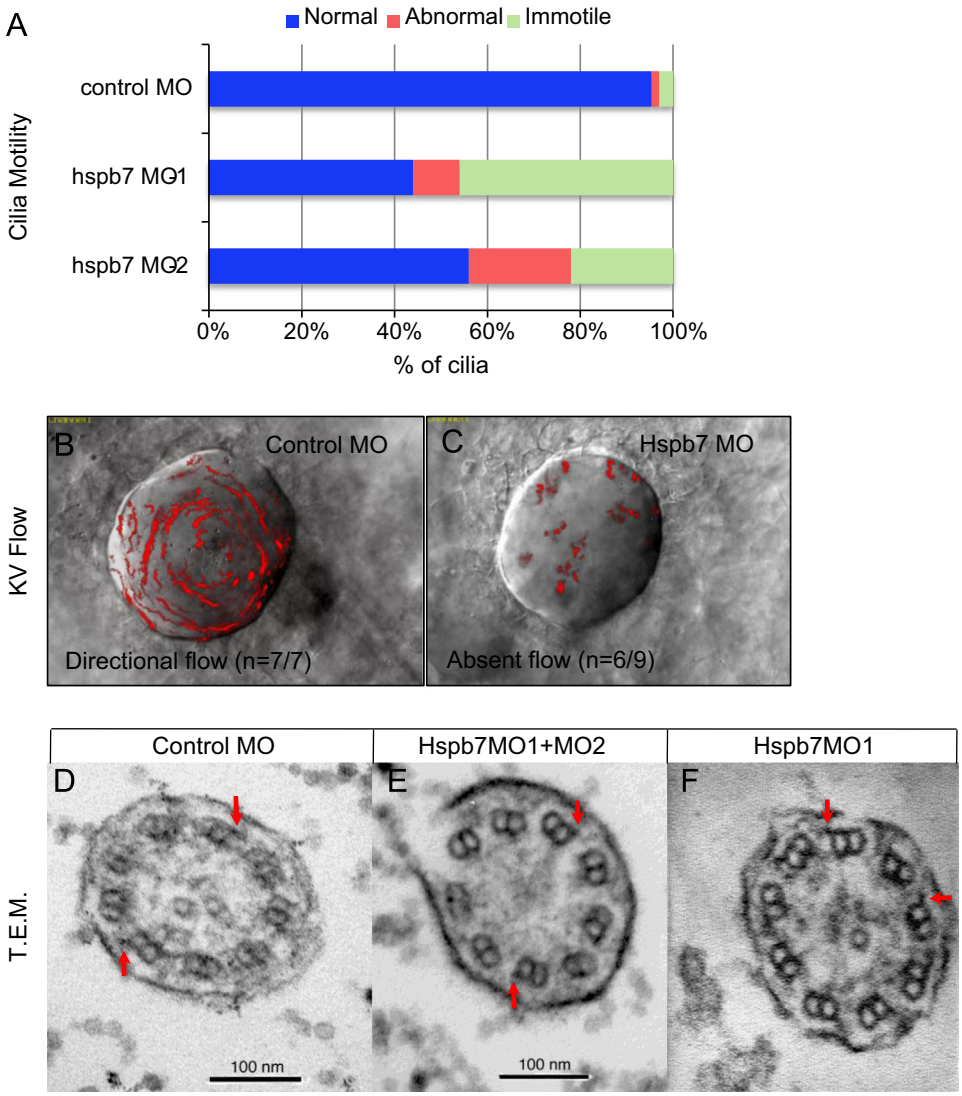

Fig. 7. *hspb7* knockdown disrupts cilia motility and asymmetric flow in Kupffer's vesicle. (A) Analysis of cilia motility revealed that many cilia in hspb7 MO embryos were immotile or beat abnormally relative to controls. (B–C) Maximum projections of fluorescent bead movements superimposed on images of KV. Beads moved in a counterclockwise direction in control MO embryos ($n=7/7$ embryos; B), whereas this directional flow was absent in most hspb7 MO embryos ($n=6/9$ embryos; C). (D–F) Transmission electron micrographs showing: (D) transverse section of cilium from embryo injected with control MO showing 9+2 configuration of microtubules, (E) transverse section showing 9+0 configuration of microtubules in a cilium from embryo injected with hspb7 MO1+MO2, and (F) transverse section shows the abnormal central microtubule configuration in a cilium from embryo injected with hspb7 MO1. Arrows: outer dynein arms.

In contrast, this directional flow was lost in most hspb7MO1-injected embryos ($n=6/9$), in which beads moved randomly via Brownian motion (Movie 5 and Fig. 7C). These results indicate that paralysis or abnormal motion of cilia in hspb7 MO embryos disrupts asymmetric fluid flow that is critical for normal L-R patterning.

Supplementary data associated with this article can be found in the online version at http://dx.doi.org/10.1016/j.ydbio.2013.10.009.

KV cilia central pair defect in hspb7 knockdown embryos

The abnormal or absent motion of cilia in KV suggested that there might be a defect in the ultrastructure of the cilia in embryos with reduced *hspb7*. Most KV cilia (7/8) in embryos injected with control MO had typical 9+2 configurations of microtubules within the ciliary axoneme (Fig. 7D). However, one cilium in a control embryo lacked a central pair, confirming that both 9+0 and 9+2 cilia exist in the zebrafish KV (Gao et al., 2010). In contrast, all cilia (10/10) in hspb7 MO1+MO2 injected embryos lacked a central pair (Fig. 7E). In addition, a cilium with a single central microtubule was detected in an hspb7MO1 injected embryo (Fig. 7G), which has a lower degree of knockdown. Outer dynein arms were present in all cilia, whether or not there was a central pair. The loss of the central pair may account for the immotility of cilia in *hspb7* morphant embryos.

Discussion

This work illustrates a role for two small heat shock proteins in supporting the establishment of laterality and the fusion of the bilateral heart fields in zebrafish through roles in Kupffer's vesicle and the yolk syncitial layer.

Role of hspb7 in laterality

Knockdown experiments with two splice-blocking morpholino oligonucleotides against *hspb7* revealed that it is required for the establishment of left–right asymmetry of the heart, gut and brain (Fig. 2A; Tables 1 and 2). A third MO targeted to the AUG site of *hspb7* (kindly shared by Gabriel Musso and Calum MacRae produced similar rates of laterality disruptions. The high degree of concordance between the direction of asymmetry in the three organs (Tables 1 and 2) is consistent with a disruption of the global vector of asymmetry at the level of KV (Amack and Yost, 2004; Chen et al., 2001; Essner et al., 2005). Although KV appeared morphologically normal, the majority of the cilia were paralyzed or moved abnormally in *hspb7* morphants (Fig. 7A–C). *hspb7* expression was never detected in otic vesicles or intermediate mesoderm; therefore it is not surprising that *hspb7* knockdown embryos did not develop other hallmarks of cilia dysfunction such as supernumerary otoliths or enlarged nephric ducts. The timing and location of *hspb7* expression in KV at the 1–4 somite period (Fig. 1D) is consistent with a role in establishing cilia function (Amack et al., 2007).

Knockdown of *hspb7* altered the ultrastructure of KV cilia. A 9+2 axoneme structure is found in the motile cilia that comprise the majority of KV cilia (Kreiling et al., 2007), although 9+0 cilia are also present (Afzelius, 2004; Fisch and Dupuis-Williams, 2011; Gao et al., 2010). In hspb7MO1+MO2 embryos all of the ciliary axonemes analyzed had 9+0 structure (Fig. 7E). In the milder hspb7MO1 knockdown, the loss of one of the central pair of microtubules was observed (Fig. 7F). These anomalous structures may account for the motility impairments in KV cilia of the hspb7MO1 knockdown embryos (Fig. 7A–C).

This finding raises the question of how *hspb7* influences the structure of the ciliary axoneme. The small heat shock proteins have a diverse set of cellular functions, and regulate cytoskeletal dynamics, protein aggregation and redox states even under conditions that do not provoke cellular stress (Boncoraglio et al., 2012; Christians et al., 2012; Sun and MacRae, 2005; Wettstein et al., 2012). Hspb7 prevents assembly of F-actin, conferring a cardioprotective activity by preventing RhoA-GTPase remodeling of the actin cytoskeleton (Ke et al., 2011), and other members of the sHsp family also regulate actin assembly (Sun and MacRae, 2005). Actin dynamics govern cilia outgrowth in KV (May-Simera et al., 2010; Ravanelli and Klingensmith, 2011). Thus a link between Hspb7 and the actin cytoskeleton is one possible mechanism for its effect on KV cilia structure. A yeast two-hybrid screen identified Filamin A, a protein that links actin to integrins, as a binding partner for human HSPB7 (Krief et al., 1999; Zhou et al., 2010). These data suggest avenues for further investigation of the molecular mechanisms of the developmental effects of sHsps.

hspb7 knockdown led to bilateral expression of *southpaw* (Fig. 4A–C). This result is consistent with a requirement for *hspb7* in KV cilia motility. Mutations and mRNA knockdowns that disrupt KV cilia motility prevent the restriction of *spaw* to the left lateral plate mesoderm (Bisgrove et al., 2012; Bisgrove et al., 2005; Kishimoto et al., 2008; Ravanelli and Klingensmith, 2011; Schottenfeld et al., 2007; Serluca et al., 2009). The self-propagation of *spaw* expression (Long et al., 2003; Wang and Yost, 2008) is checked at its midline, anterior and posterior borders by multiple barriers: antagonism by *lefty1* in notochord (Meno et al., 1998; Nakamura et al., 2006), by *lefty2* in the heart field (Lenhart et al., 2011), by both *charon* in the peri-KV region at 8 somite stage (Hashimoto et al., 2004; Lopes et al., 2010; Matsui and Bessho, 2012) and by competition between the BMP and Nodal pathways for their common downstream factor Smad4 (Furtado et al., 2008). Knockdown of *hspb7* derepresses *spaw* expression in the right lateral plate, but does not disrupt these midline barriers to *spaw* expansion (Fig. 4A and C); *lefty1* in the notochord is intact, and the anterior and posterior extent of *spaw* are normal. Disruption of the midline barriers would result in discordant asymmetry (Bisgrove et al., 2000; Chin et al., 2000; Lenhart et al., 2011). However, there is a high degree of concordance between heart, gut and brain laterality in *hspb7* morphants (Tables 1 and 2), indicating that *hspb7* is not necessary for the integrity of the midline.

Genes downstream of *spaw* in the laterality cascade – *lefty1* in brain, *lefty2* in heart, and *pitx2* in the left lateral plate (Long et al., 2003) – are also abnormally expressed in *hspb7* morphants (Fig. 4F–I). Although *spaw* becomes primarily bilateral, the majority of *hspb7* knockdown embryos express the downstream genes on either the left or right. This resolution from bilateral *spaw* to a mixture of right, left, and bilateral *pitx2*, *lefty1* and *lefty2* is similar to that observed with other laterality mutants and morphants (Hashimoto et al., 2004; Hatler et al., 2009; Lin and Xu, 2009; Schottenfeld et al., 2007). Because the rate of anterior expansion of *spaw* determines the direction of asymmetry, this is a potential mechanism for resolving bilaterally symmetric *spaw* expression to unilateral (although randomized) expression of the downstream genes (Wang and Yost, 2008). In summary, these results indicate that *hspb7* is required in KV to support cilia motility (Fig. 8A), which is required for repression of *spaw* on the right, and restriction of the downstream genes *pitx2*, *lefty1* and *lefty2* to the left side.

hspb12 and laterality

hspb12 knockdown appears to have comparable effects on zebrafish laterality to those of *hspb7* knockdown, although with

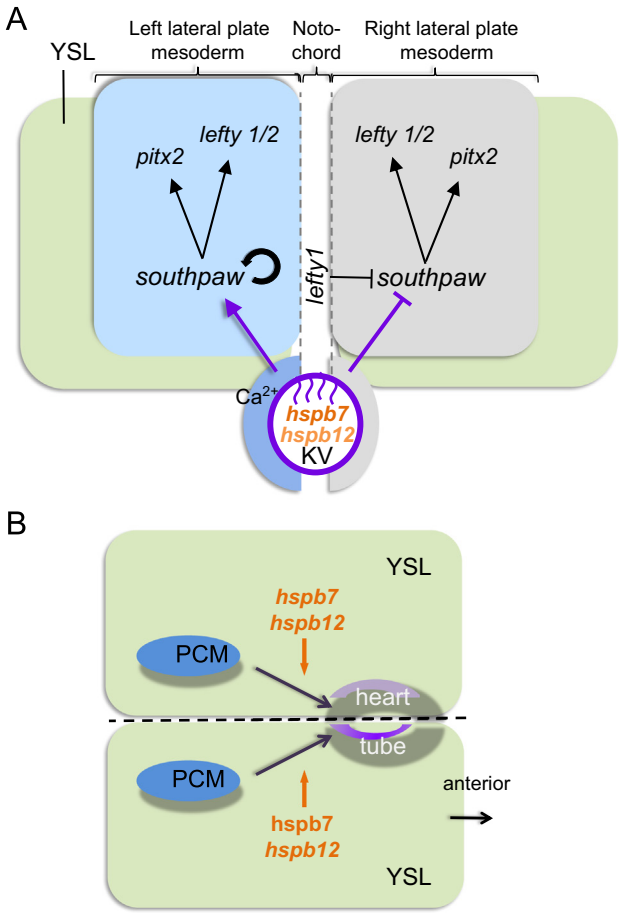

Fig. 8. Model for *hspb7* and *hspb12* function. (A) Mechanism of small heat shock proteins in laterality determination. Hspb7 protein is required for KV cilia motility, which leads to the upregulation of Ca^{2+} to the left of the node. This signal is propagated to the lateral plate mesoderm, where *spaw* expression expands in a positive feedback loop. Loss of *hspb7* expression leads to impaired cilia motility, derepressing *spaw* on the right. *hspb12* plays a supportive role in KV, which is revealed when *hspb7* is reduced. (B) *hspb7* and *hspb12* in the YSL are necessary for the migration of the precardiac mesoderm (PCM). Reduction of *hspb7* and *hspb12* specifically in yolk inhibits subsequent migration of the precardiac mesoderm to the midline, causing cardia bifida.

lower penetrance (Figs. 2 and 3A). Reduction of *hspb12* mRNA perturbs *pitx2*, *lefty1* and *lefty2* expression (Fig. 5D, E, and I); the dependence of *spaw* on *hspb12* depends upon the genetic background. Co-injection of sub-optimal doses of hsp7MO1 and hspb12MO1 induce a higher proportion of right and failed (midline) heart jogs than either MO alone (Fig. 3C). Although *hspb12* was not detected in KV in embryos of the AB line, it is likely that it is expressed in KV at low levels, which may vary by strain. Therefore, *hspb12* may play a supporting role in KV cilia function (Fig. 8A), which is primarily revealed when *hspb7* is reduced. Hspb7 forms homo-multimers with up to 12 subunits (Yang et al., 2011), and it interacts with at least one other sHsp, Hspb8 (Sun et al., 2004). Hspb7–Hspb12 binding has not been studied because mammals lack *hspb12*, but they are plausible binding partners due to the homology of the α-crystallin domains. These results demonstrate redundancy between *hspb7* and *hspb12* in the laterality gene cascade.

There are some intriguing differences between *hspb7* and *hspb12*. In *hspb12* deficient embryos, the pattern of *pitx2* expression differs from that of *lefty1* and *lefty2*. Although ectopic *pitx2* may be expressed on the left, bilaterally, or on the right (Fig. 5D), *lefty1* and *lefty2* are expressed on the left, bilaterally or are completely absent (Fig. 5E, I) in *hspb12* morphants; *lefty1* and *lefty2* are never expressed on the right side alone. *pitx2* is regulated not only by *spaw* but also by Bmp activity in the peri-KV region (Chocron et al., 2007). *bmp4* expression near the node is normal in *hspb12* knockdown embryos (data not shown). The heart and brain expression of *lefty2* and *lefty1* are largely concordant in *hspb12* knockdown embryos; however, the heart and gut laterality are more frequently discordant (Table 2). The disparity between the *lefty* genes and gut migration may stem from the fact that only *pitx2* is expressed in the gut precursors, and we observed that *pitx2* expression levels are somewhat reduced in *hspb12* morphants. In addition, *hspb12* may support the migration necessary for the heart to jog at 26 hpf, and therefore the disparity between heart and gut migration may be due to a late failure of heart migration rather than uncoupling of heart and gut laterality. Taken together, these results suggest that *hspb12* has functions in establishing laterality that do not entirely duplicate those of *hspb7*.

hspb7, hspb12, and heart migration

In addition to a role in KV cilia motility, *hspb7* is also necessary to support migration of precardiac mesoderm along the YSL. Although a mild knockdown of *hspb7* causes laterality defects (Fig. 2A), a strong knockdown to 12% of control levels (Fig. 2F; Supplementary Fig. 1) causes cardia bifida and retards cardiac precursor migration (Fig. 2G–J). *hspb7* is expressed both in YSL from 6–12 hpf, and in the migrating precardiac mesoderm from the 12 somite stage (Fig. 1A–D). To clarify which expression domain is responsible for the laterality and migration defects, we injected morpholino into the yolk between 3 and 4 hpf. Yolk injections restrict the MO to cells adjacent to the yolk, including the YSL. This injection method does not permit any MO to reach the embryo proper (Amack and Yost, 2004; Arrington and Yost, 2009; Essner et al., 2005). Yolk targeting of the combined hspb7MO1 and hspb7MO2 is sufficient to cause cardia bifida (Fig. 2K), indicating that the failure of precursors to migrate is due to a requirement for *hspb7* in the YSL rather than in the precardiac mesoderm (Fig. 8B).

In strong *hspb7* morphants there is clearly a defect in the migration of cardiac precursors to the midline at the 18–20 somite stage. In yolk-injected *hspb7* morphants that do form a fused heart tube, the failure of the atrial end of the heart to jog left by 26 somites may also be due to a migration defect, in this case blocking migration away from the midline. In the more sensitive Tg(cmlc:GFP) × WT line, yolk injection of hspb12MO also causes a small amount of cardia bifida (8.7% vs. 0% of control), and slows anterior migration (Supplementary Fig. 2).

Together these lines of evidence indicate that *hspb7*, and to a lesser extent *hspb12*, are important in making the YSL capable of supporting precardiac mesoderm migration (Fig. 8B). YSL-specific knockdowns and mutations have previously demonstrated that the YSL drives cardiac migration, through a common pathway that promotes fibronectin expression in the heart field (Arrington and Yost, 2009; Kupperman et al., 2000; Matsui et al., 2007; Osborne et al., 2008; Sakaguchi et al., 2006; Trinh and Stainier, 2004). Notably, knockdown of the small heat shock protein *hspb1* (*hsp27*) results in cardia bifida in *Xenopus* (Brown et al., 2007), although it does not do so in zebrafish (Tucker et al., 2009). We confirmed that a second *hspb1* MO translation-blocking MO did not affect laterality or heart fusion (MJM and LDH, unpublished data). In zebrafish, *hspb7* may fill the role of *hspb1* in *Xenopus*, despite their limited homology outside the α-crystallin domain (Elicker and Hutson, 2007).

Inability to rescue hspb7 and hspb12 morphants

Surprisingly, neither whole embryo nor yolk-specific replacement of *hspb7* or *hspb12* mRNA was sufficent to rescue the *hspb7*

or *hspb12* morphants. We were unable to detect an alternative transcript of *hspb7*, suggesting that we had the only transcript present in the early zebrafish embryo. The constructs were expressed in cultured cells, the injected mRNA survived in embryos at least 24 h, and injected β-galactosidase RNA was targeted to the whole embryo or yolk as expected. It is possible that post-transcriptional modifications to the RNA, or a very specific pattern of expression is necessary to obtain rescue of the *hspb7* and *hspb12* morphants.

This work demonstrates that *hspb7* and *hspb12* have partially overlapping roles in establishing embryonic lateral asymmetry in the zebrafish embryo through their effects on Kupffer's vesicle and the downstream laterality genes. We show that *hspb7* is necessary for the presence of the central pair of microtubules in the motile cilia in Kupffer's vesicle. Furthermore, both *hspb7* and *hspb12* support the migration of the heart precursors to the midline through a role in the yolk syncitial layer. These findings add to a growing list of developmental roles for small heat shock proteins.

Note added in proof: While this manuscript was in revision, an independent group reported similar findings, in which *hspb7* caused laterality defects, cardia bifida, and heart morphogenesis defects (Rosenfeld et al., 2013). In contrast, they found that *hspb12* promoted only heart morphogenesis defects but did not disrupt laterality determination. The strain-dependence of *hspb12* morpholino activity suggests that this contrast is due to variations in the activity of *hspb12* in KV between strains. These authors also found that *hspb7* RNA promoted a small statistical improvement but did not substantially rescue *hspb7* morpholino phenotypes.

Acknowledgments

We are grateful to Nancy Piatczyk for expert T.E.M. assistance, to Lois Banta for comments on the manuscript, to Ashley Ngo for help with in situs, and to Gabriel Musso and Calum MacRae for sharing data before publication. This research was supported by Williams College, the Essel Foundation (LDH and MJM), the Groff Foundation (MJM) and NHLBI R01HL095690 (J.D.A.).

Appendix A. Supporting information

Supplementary data associated with this article can be found in the online version at http://dx.doi.org/10.1016/j.ydbio.2013.10.009.

References

Afzelius, B.A., 2004. Cilia-related diseases. J. Pathol. 204, 470–477.
Alexander, J., Rothenberg, M., Henry, G.L., Stainier, D.Y., 1999. *Casanova* plays an early and essential role in endoderm formation in zebrafish. Dev. Biol. 215, 343–357.
Amack, J.D., Wang, X., Yost, H.J., 2007. Two T-box genes play independent and cooperative roles to regulate morphogenesis of ciliated Kupffer's vesicle in zebrafish. Dev. Biol. 310, 196–210.
Amack, J.D., Yost, H.J., 2004. The T box transcription factor no tail in ciliated cells controls zebrafish left-right asymmetry. Curr. Biol. 14, 685–690.
Arrington, C.B., Yost, H.J., 2009. Extra-embryonic syndecan 2 regulates organ primordia migration and fibrillogenesis throughout the zebrafish embryo. Development 136, 3143–3152.
Aw, S., Adams, D.S., Qiu, D., Levin, M., 2008. H,K-ATPase protein localization and Kir4.1 function reveal concordance of three axes during early determination of left-right asymmetry. Mech. Dev. 125, 353–372.
Beyer, T., Danilchik, M., Thumberger, T., Vick, P., Tisler, M., Schneider, I., Bogusch, S., Andre, P., Ulmer, B., Walentek, P., Niesler, B., Blum, M., Schweickert, A., 2012. Serotonin signaling is required for Wnt-dependent GRP specification and leftward flow in *Xenopus*. Curr. Biol. 22, 33–39.
Bisgrove, B.W., Essner, J.J., Yost, H.J., 1999. Regulation of midline development by antagonism of lefty and nodal signaling. Development 126, 3253–3262.
Bisgrove, B.W., Essner, J.J., Yost, H.J., 2000. Multiple pathways in the midline regulate concordant brain, heart and gut left-right asymmetry. Development 127, 3567–3579.
Bisgrove, B.W., Makova, S., Yost, H.J., Brueckner, M., 2012. RFX2 is essential in the ciliated organ of asymmetry and an RFX2 transgene identifies a population of ciliated cells sufficient for fluid flow. Dev. Biol. 363, 166–178.
Bisgrove, B.W., Morelli, S.H., Yost, H.J., 2003. Genetics of human laterality disorders: insights from vertebrate model systems. Ann. Rev. Genomics Hum. Genet. 4, 1–32.
Bisgrove, B.W., Snarr, B.S., Emrazian, A., Yost, H.J., 2005. Polaris and Polycystin-2 in dorsal forerunner cells and Kupffer's vesicle are required for specification of the zebrafish left–right axis. Dev. Biol. 287, 274–288.
Boncoraglio, A., Minoia, M., Carra, S., 2012. The family of mammalian small heat shock proteins (HSPBs): implications in protein deposit diseases and motor neuropathies. Int. J. Biochem. Cell Biol. 44, 1657–1669.
Bozzola, J.J., Russell, L.D., 1992. Electron Microscopy: Principles and Techniques for Biologists. Jones and Bartlett Learning, Boston.
Brown, D.D., Christine, K.S., Showell, C., Conlon, F.L., 2007. Small heat shock protein Hsp27 is required for proper heart tube formation. Genesis 45, 667–678.
Buceta, J., Ibanes, M., Rasskin-Gutman, D., Okada, Y., Hirokawa, N., Izpisua-Belmonte, J.C., 2005. Nodal cilia dynamics and the specification of the left/right axis in early vertebrate embryo development. Biophys. J. 89, 2199–2209.
Burns, C.G., Milan, D.J., Grande, E.J., Rottbauer, W., MacRae, C.A., Fishman, M.C., 2005. High-throughput assay for small molecules that modulate zebrafish embryonic heart rate. Nat. Chem. Biol. 1, 263–264.
Campione, M., Steinbeisser, H., Schweickert, A., Deissler, K., van Bebber, F., Lowe, L. A., Nowotschin, S., Viebahn, C., Haffter, P., Kuehn, M.R., Blum, M., 1999. The homeobox gene *Pitx2*: mediator of asymmetric left-right signaling in vertebrate heart and gut looping. Development 126, 1225–1234.
Cartwright, J.H., Piro, O., Tuval, I., 2004. Fluid-dynamical basis of the embryonic development of left-right asymmetry in vertebrates. Proc. Nat. Acad. Sci. USA 101, 7234–7239.
Chen, J.N., van Bebber, F., Goldstein, A.M., Serluca, F.C., Jackson, D., Childs, S., Serbedzija, G., Warren, K.S., Mably, J.D., Lindahl, P., Mayer, A., Haffter, P., Fishman, M.C., 2001. Genetic steps to organ laterality in zebrafish. Comp. Funct. Genomics 2, 60–68.
Chin, A.J., Tsang, M., Weinberg, E.S., 2000. Heart and gut chiralities are controlled independently from initial heart position in the developing zebrafish. Dev. Biol. 227, 403–421.
Chocron, S., Verhoeven, M.C., Rentzsch, F., Hammerschmidt, M., Bakkers, J., 2007. Zebrafish Bmp4 regulates left–right asymmetry at two distinct developmental time points. Dev. Biol. 305, 577–588.
Christians, E.S., Ishiwata, T., Benjamin, I.J., 2012. Small heat shock proteins in redox metabolism: implications for cardiovascular diseases. Int. J. Biochem. Cell Biol. 44, 1632–1645.
Dickmeis, T., Mourrain, P., Saint-Etienne, L., Fischer, N., Aanstad, P., Clark, M., Strahle, U., Rosa, F., 2001. A crucial component of the endoderm formation pathway, CASANOVA, is encoded by a novel sox-related gene. Genes Dev. 15, 1487–1492.
Doran, P., Gannon, J., O'Connell, K., Ohlendieck, K., 2007. Aging skeletal muscle shows a drastic increase in the small heat shock proteins alphaB-crystallin/HspB5 and cvHsp/HspB7. Eur. J. Cell Biol. 86, 629–640.
Doran, P., Martin, G., Dowling, P., Jockusch, H., Ohlendieck, K., 2006. Proteome analysis of the dystrophin-deficient MDX diaphragm reveals a drastic increase in the heat shock protein cvHSP. Proteomics 6, 4610–4621.
Draper, B.W., Morcos, P.A., Kimmel, C.B., 2001. Inhibition of zebrafish *fgf8* pre-mRNA splicing with morpholino oligos: a quantifiable method for gene knockdown. Genesis 30, 154–156.
Elicker, K.S., Hutson, L.D., 2007. Genome-wide analysis and expression profiling of the small heat shock proteins in zebrafish. Gene 403, 60–69.
Essner, J.J., Amack, J.D., Nyholm, M.K., Harris, E.B., Yost, H.J., 2005. Kupffer's vesicle is a ciliated organ of asymmetry in the zebrafish embryo that initiates left–right development of the brain, heart and gut. Development 132, 1247–1260.
Essner, J.J., Branford, W.W., Zhang, J., Yost, H.J., 2000. Mesendoderm and left–right brain, heart and gut development are differentially regulated by *pitx2* isoforms. Development 127, 1081–1093.
Fisch, C., Dupuis-Williams, P., 2011. Ultrastructure of cilia and flagella – back to the future!. Biol. Cell 103, 249–270.
Flanagan-Steet, H., Fox, M.A., Meyer, D., Sanes, J.R., 2005. Neuromuscular synapses can form in vivo by incorporation of initially aneural postsynaptic specializations. Development 132, 4471–4481.
Francescatto, L., Rothschild, S.C., Myers, A.L., Tombes, R.M., 2010. The activation of membrane targeted CaMK-II in the zebrafish Kupffer's vesicle is required for left–right asymmetry. Development 137, 2753–2762.
Fujita, Y., Ohto, E., Katayama, E., Atomi, Y., 2004. alphaB-crystallin-coated MAP microtubule resists nocodazole and calcium-induced disassembly. J. Cell Sci. 117, 1719–1726.
Fukumoto, T., Kema, I.P., Levin, M., 2005. Serotonin signaling is a very early step in patterning of the left-right axis in chick and frog embryos. Curr. Biol. 15, 794–803.
Furtado, M.B., Solloway, M.J., Jones, V.J., Costa, M.W., Biben, C., Wolstein, O., Preis, J.I., Sparrow, D.B., Saga, Y., Dunwoodie, S.L., Robertson, E.J., Tam, P.P., Harvey, R.P., 2008. BMP/SMAD1 signaling sets a threshold for the left/right pathway in lateral plate mesoderm and limits availability of SMAD4. Genes Dev. 22, 3037–3049.

Gamse, J.T., Kuan, Y.S., Macurak, M., Brosamle, C., Thisse, B., Thisse, C., Halpern, M.E., 2005. Directional asymmetry of the zebrafish epithalamus guides dorsoventral innervation of the midbrain target. Development 132, 4869–4881.
Gao, C., Wang, G., Amack, J.D., Mitchell, D.R., 2010. Oda16/Wdr69 is essential for axonemal dynein assembly and ciliary motility during zebrafish embryogenesis. Dev. Dyn. 239, 2190–2197.
Glickman, N.S., Yelon, D., 2002. Cardiac development in zebrafish: coordination of form and function. Semin. Cell Dev. Biol. 13, 507–513.
Golenhofen, N., Perng, M.D., Quinlan, R.A., Drenckhahn, D., 2004. Comparison of the small heat shock proteins alphaB-crystallin, MKBP, HSP25, HSP20, and cvHSP in heart and skeletal muscle. Histochem. Cell Biol. 122, 415–425.
Hashimoto, H., Rebagliati, M., Ahmad, N., Muraoka, O., Kurokawa, T., Hibi, M., Suzuki, T., 2004. The Cerberus/Dan-family protein Charon is a negative regulator of Nodal signaling during left-right patterning in zebrafish. Development 131, 1741–1753.
Hatler, J.M., Essner, J.J., Johnson, R.G., 2009. A gap junction connexin is required in the vertebrate left-right organizer. Dev. Biol. 336, 183–191.
Hirokawa, N., Okada, Y., Tanaka, Y., 2009. Fluid dynamic mechanism responsible for breaking the left–right symmetry of the human body: the nodal flow. Annu. Rev. Fluid Mech. 41, 53–72.
Horne-Badovinac, S., Rebagliati, M., Stainier, D.Y., 2003. A cellular framework for gut-looping morphogenesis in zebrafish. Science 302, 662–665.
Houck, S.A., Clark, J.I., 2010. Dynamic subunit exchange and the regulation of microtubule assembly by the stress response protein human alphaB crystallin. PLoS ONE 5, e11795.
Kawakami, Y., Raya, A., Raya, R.M., Rodriguez-Esteban, C., Belmonte, J.C., 2005. Retinoic acid signalling links left-right asymmetric patterning and bilaterally symmetric somitogenesis in the zebrafish embryo. Nature 435, 165–171.
Ke, L., Meijering, R.A.M., Hoogstra-Berends, F., Mackovicova, K., Vos, M.J., Van Gelder, I.C., Henning, R.H., Kampinga, H.H., Brundel, B.J.J.M., 2011. HSPB1, HSPB6, HSPB7 and HSPB8 Protect against RhoA GTPase-Induced Remodeling in Tachypaced Atrial Myocytes. PLoS ONE 6, e20395.
Kikuchi, Y., Agathon, A., Alexander, J., Thisse, C., Waldron, S., Yelon, D., Thisse, B., Stainier, D.Y.R., 2001. Casanova encodes a novel Sox-related protein necessary and sufficient for early endoderm formation in zebrafish. Genes Dev. 15, 1493–1505.
Kimmel, C.B., Ballard, W.W., Kimmel, S.R., Ullmann, B., Schilling, T.F., 1995. Stages of embryonic development of the zebrafish. Dev. Dyn. 203, 253–310.
Kimmel, C.B., Law, R.D., 1985. Cell lineage of zebrafish blastomeres. II. Formation of the yolk syncytial layer. Dev. Biol. 108, 86–93.
Kishimoto, N., Cao, Y., Park, A., Sun, Z., 2008. Cystic kidney gene seahorse regulates cilia-mediated processes and Wnt pathways. Dev. Cell 14, 954–961.
Kramer-Zucker, A.G., Olale, F., Haycraft, C.J., Yoder, B.K., Schier, A.F., Drummond, I.A., 2005. Cilia-driven fluid flow in the zebrafish pronephros, brain and Kupffer's vesicle is required for normal organogenesis. Development 132, 1907–1921.
Kreiling, J.A., Williams, G., Creton, R., 2007. Analysis of Kupffer's vesicle in zebrafish embryos using a cave automated virtual environment. Dev. Dyn. 236, 1963–1969.
Krief, S., Faivre, J.F., Robert, P., Le Douarin, B., Brument-Larignon, N., Lefrere, I., Bouzyk, M.M., Anderson, K.M., Greller, L.D., Tobin, F.L., Souchet, M., Bril, A., 1999. Identification and characterization of cvHsp. A novel human small stress protein selectively expressed in cardiovascular and insulin-sensitive tissues. J. Biol. Chem. 274, 36592–36600.
Kupperman, E., An, S., Osborne, N., Waldron, S., Stainier, D.Y., 2000. A sphingosine-1-phosphate receptor regulates cell migration during vertebrate heart development. Nature 406, 192–195.
Kurpios, N.A., Ibanes, M., Davis, N.M., Lui, W., Katz, T., Martin, J.F., Izpisua Belmonte, J.C., Tabin, C.J., 2008. The direction of gut looping is established by changes in the extracellular matrix and in cell:cell adhesion. Proc. Nat. Acad. Sci. USA 105, 8499–8506.
Lenhart, K.F., Lin, S.Y., Titus, T.A., Postlethwait, J.H., Burdine, R.D., 2011. Two additional midline barriers function with midline *lefty1* expression to maintain asymmetric nodal signaling during left–right axis specification in zebrafish. Development 138, 4405–4410.
Levin, M., Johnson, R.L., Stern, C.D., Kuehn, M., Tabin, C., 1995. A molecular pathway determining left–right asymmetry in chick embryogenesis. Cell 82, 803–814.
Levin, M., Thorlin, T., Robinson, K.R., Nogi, T., Mercola, M., 2002. Asymmetries in H^+/K^+-ATPase and cell membrane potentials comprise a very early step in left–right patterning. Cell 111, 77–89.
Lin, X., Xu, X., 2009. Distinct functions of Wnt/beta-catenin signaling in KV development and cardiac asymmetry. Development 136, 207–217.
Long, S., Ahmad, N., Rebagliati, M., 2003. The zebrafish *nodal*-related gene *southpaw* is required for visceral and diencephalic left–right asymmetry. Development 130, 2303–2316.
Lopes, S.S., Lourenco, R., Pacheco, L., Moreno, N., Kreiling, J., Saude, L., 2010. Notch signalling regulates left–right asymmetry through ciliary length control. Development 137, 3625–3632.
Lowe, L.A., Supp, D.M., Sampath, K., Yokoyama, T., Wright, C.V., Potter, S.S., Overbeek, P., Kuehn, M.R., 1996. Conserved left–right asymmetry of nodal expression and alterations in murine situs inversus. Nature 381, 158–161.
Marvin, M., O'Rourke, D., Kurihara, T., Juliano, C.E., Harrison, K.L., Hutson, L.D., 2008. Developmental expression patterns of the zebrafish small heat shock proteins. Dev. Dyn. 237, 454–463.
Matkovich, S.J., Van Booven, D.J., Hindes, A., Kang, M.Y., Druley, T.E., Vallania, F.L., Mitra, R.D., Reilly, M.P., Cappola, T.P., Dorn II, G.W., 2010. Cardiac signaling genes exhibit unexpected sequence diversity in sporadic cardiomyopathy, revealing HSPB7 polymorphisms associated with disease. J. Clin. Invest. 120, 280–289.
Matsui, T., Bessho, Y., 2012. Left-right asymmetry in zebrafish. Cell. Mol. Life Sci. 69, 3069–3077.
Matsui, T., Raya, A., Callol-Massot, C., Kawakami, Y., Oishi, I., Rodriguez-Esteban, C., Belmonte, J.C., 2007. *miles-apart*-Mediated regulation of cell-fibronectin interaction and myocardial migration in zebrafish. Nat. Clin. Pract. Cardiovasc. Med. 4 (Suppl. 1), S77–S82.
May-Simera, H.L., Kai, M., Hernandez, V., Osborn, D.P., Tada, M., Beales, P.L., 2010. Bbs8, together with the planar cell polarity protein Vangl2, is required to establish left–right asymmetry in zebrafish. Dev. Biol. 345, 215–225.
Meno, C., Ito, Y., Saijoh, Y., Matsuda, Y., Tashiro, K., Kuhara, S., Hamada, H., 1997. Two closely-related left-right asymmetrically expressed genes, *lefty-1* and *lefty-2*: their distinct expression domains, chromosomal linkage and direct neuralizing activity in *Xenopus* embryos. Genes Cells 2, 513–524.
Meno, C., Saijoh, Y., Fujii, H., Ikeda, M., Yokoyama, T., Yokoyama, M., Toyoda, Y., Hamada, H., 1996. Left–right asymmetric expression of the TGF beta-family member *lefty* in mouse embryos. Nature 381, 151–155.
Meno, C., Shimono, A., Saijoh, Y., Yashiro, K., Mochida, K., Ohishi, S., Noji, S., Kondoh, H., Hamada, H., 1998. *lefty-1* is required for left–right determination as a regulator of *lefty-2* and *nodal*. Cell 94, 287–297.
Musso G., Tasan M., Mosimann C., Beaver J.E., Plovie E., Carr L.A., Chua H.N., Dunham J., Zuberi K., Rodriguez H., Morris Q., Zon L., Roth F.P., MacRae C., Novel cardiovascular gene functions revealed via systematic phenotype prediction in zebrafish, *Development*, in press.
Nakamura, T., Mine, N., Nakaguchi, E., Mochizuki, A., Yamamoto, M., Yashiro, K., Meno, C., Hamada, H., 2006. Generation of robust left–right asymmetry in the mouse embryo requires a self-enhancement and lateral-inhibition system. Dev. Cell 11, 495–504.
Nonaka, S., Shiratori, H., Saijoh, Y., Hamada, H., 2002. Determination of left–right patterning of the mouse embryo by artificial nodal flow. Nature 418, 96–99.
Nonaka, S., Yoshiba, S., Watanabe, D., Ikeuchi, S., Goto, T., Marshall, W.F., Hamada, H., 2005. De novo formation of left–right asymmetry by posterior tilt of nodal cilia. PLoS Biol. 3, e268.
Okada, Y., Nonaka, S., Tanaka, Y., Saijoh, Y., Hamada, H., Hirokawa, N., 1999. Abnormal nodal flow precedes situs inversus in iv and inv mice. Mol. Cell 4, 459–468.
Olbrich, H., Haffner, K., Kispert, A., Volkel, A., Volz, A., Sasmaz, G., Reinhardt, R., Hennig, S., Lehrach, H., Konietzko, N., Zariwala, M., Noone, P.G., Knowles, M., Mitchison, H.M., Meeks, M., Chung, E.M., Hildebrandt, F., Sudbrak, R., Omran, H., 2002. Mutations in DNAH5 cause primary ciliary dyskinesia and randomization of left–right asymmetry. Nat. Genet. 30, 143–144.
Osborne, N., Brand-Arzamendi, K., Ober, E.A., Jin, S.W., Verkade, H., Holtzman, N.G., Yelon, D., Stainier, D.Y., 2008. The spinster homolog, two of hearts, is required for sphingosine 1-phosphate signaling in zebrafish. Curr. Biol. 18, 1882–1888.
Ramsdell, A.F., 2005. Left–right asymmetry and congenital cardiac defects: getting to the heart of the matter in vertebrate left-right axis determination. Dev. Biol. 288, 1–20.
Ravanelli, A.M., Klingensmith, J., 2011. The actin nucleator Cordon-bleu is required for development of motile cilia in zebrafish. Dev. Biol. 350, 101–111.
Raya, A., Belmonte, J.C., 2006. Left–right asymmetry in the vertebrate embryo: from early information to higher-level integration. Nat. Rev. Genet. 7, 283–293.
Rosenfeld, G.E., Mercer, E.J., Mason, C.E., Evans, T., 2013. Small heat shock proteins Hspb7 and Hspb12 regulate early steps of cardiac morphogenesis. Dev. Biol. 381, :389–400.
Saijoh, Y., Adachi, H., Sakuma, R., Yeo, C.Y., Yashiro, K., Watanabe, M., Hashiguchi, H., Mochida, K., Ohishi, S., Kawabata, M., Miyazono, K., Whitman, M., Hamada, H., 2000. Left–right asymmetric expression of *lefty2* and *nodal* is induced by a signaling pathway that includes the transcription factor FAST2. Mol. Cell 5, 35–47.
Sakaguchi, T., Kikuchi, Y., Kuroiwa, A., Takeda, H., Stainier, D.Y., 2006. The yolk syncytial layer regulates myocardial migration by influencing extracellular matrix assembly in zebrafish. Development 133, 4063–4072.
Schottenfeld, J., Sullivan-Brown, J., Burdine, R.D., 2007. Zebrafish *curly up* encodes a Pkd2 ortholog that restricts left-side-specific expression of *southpaw*. Development 134, 1605–1615.
Schweickert, A., Weber, T., Beyer, T., Vick, P., Bogusch, S., Feistel, K., Blum, M., 2007. Cilia-driven leftward flow determines laterality in *Xenopus*. Curr. Biol. 17, 60–66.
Serluca, F.C., Xu, B., Okabe, N., Baker, K., Lin, S.Y., Sullivan-Brown, J., Konieczkowski, D.J., Jaffe, K.M., Bradner, J.M., Fishman, M.C., Burdine, R.D., 2009. Mutations in zebrafish leucine-rich repeat-containing six-like affect cilia motility and result in pronephric cysts, but have variable effects on left-right patterning. Development 136, 1621–1631.
Shiratori, H., Sakuma, R., Watanabe, M., Hashiguchi, H., Mochida, K., Sakai, Y., Nishino, J., Saijoh, Y., Whitman, M., Hamada, H., 2001. Two-step regulation of left-right asymmetric expression of *Pitx2*: initiation by nodal signaling and maintenance by Nkx2. Mol. Cell 7, 137–149.
Smith, K.A., Chocron, S., von der Hardt, S., de Pater, E., Soufan, A., Bussmann, J., Schulte-Merker, S., Hammerschmidt, M., Bakkers, J., 2008. Rotation and asymmetric development of the zebrafish heart requires directed migration of cardiac progenitor cells. Dev. Cell 14, 287–297.
Stark, K., Esslinger, U.B., Reinhard, W., Petrov, G., Winkler, T., Komajda, M., Isnard, R., Charron, P., Villard, E., Cambien, F., Tiret, L., Aumont, M.C., Dubourg, O., Trochu, J.N., Fauchier, L., Degroote, P., Richter, A., Maisch, B., Wichter, T., Zollbrecht, C., Grassl, M., Schunkert, H., Linsel-Nitschke, P., Erdmann, J., Baumert, J., Illig, T., Klopp, N., Wichmann, H.E., Meisinger, C., Koenig, W., Lichtner, P., Meitinger, T., Schillert, A., Konig, I.R., Hetzer, R., Heid, I.M., Regitz-Zagrosek, V., Hengstenberg, C.,

2010. Genetic association study identifies HSPB7 as a risk gene for idiopathic dilated cardiomyopathy. PLoS Genet. 6, e1001167.
Sun, X., Fontaine, J.M., Rest, J.S., Shelden, E.A., Welsh, M.J., Benndorf, R., 2004. Interaction of human HSP22 (HSPB8) with other small heat shock proteins. J. Biol. Chem. 279, 2394–2402.
Sun, Y., MacRae, T.H., 2005. Small heat shock proteins: molecular structure and chaperone function. Cell. Mol. Life Sci. 62, 2460–2476.
Thisse, C., Thisse, B., 2008. High-resolution in situ hybridization to whole-mount zebrafish embryos. Nat. Protoc. 3, 59–69.
Trinh, L.A., Stainier, D.Y., 2004. Fibronectin regulates epithelial organization during myocardial migration in zebrafish. Dev. Cell 6, 371–382.
Tucker, N.R., Shelden, E.A., 2009. Hsp27 associates with the titin filament system in heat-shocked zebrafish cardiomyocytes. Exp. Cell Res. 315, 3176–3186.
Tucker, N.R., Ustyugov, A., Bryantsev, A.L., Konkel, M.E., Shelden, E.A., 2009. Hsp27 is persistently expressed in zebrafish skeletal and cardiac muscle tissues but dispensable for their morphogenesis. Cell Stress Chaperones 14, 521–533.
Vos, M.J., Kanon, B., Kampinga, H.H., 2009. HSPB7 is a SC35 speckle resident small heat shock protein. Biochim. Biophys. Acta 1793, 1343–1353.
Vos, M.J., Zijlstra, M.P., Kanon, B., van Waarde-Verhagen, M.A., Brunt, E.R., Oosterveld-Hut, H.M., Carra, S., Sibon, O.C., Kampinga, H.H., 2010. HSPB7 is the most potent polyQ aggregation suppressor within the HSPB family of molecular chaperones. Hum. Mol. Genet. 19, 4677–4693.
Wang, G., Cadwallader, A.B., Jang, D.S., Tsang, M., Yost, H.J., Amack, J.D., 2011. The Rho kinase Rock2b establishes anteroposterior asymmetry of the ciliated Kupffer's vesicle in zebrafish. Development 138, 45–54.
Wang, X., Yost, H.J., 2008. Initiation and propagation of posterior to anterior (PA) waves in zebrafish left–right development. Dev. Dyn. 237, 3640–3647.
Westerfield, M., Zon, L.I., Detrich, H.W., 2009. Essential Zebrafish Methods: Genetics and Genomics. Academic Press.
Wettstein, G., Bellaye, P.S., Micheau, O., Bonniaud, P., 2012. Small heat shock proteins and the cytoskeleton: an essential interplay for cell integrity? Int. J. Biochem. Cell Biol. 44, 1680–1686.
Yang, Z., Wang, Y., Lu, Y., Zhao, X., 2011. Molecular characterization of rat cvHsp/HspB7 in vitro and its dynamic molecular architecture. Mol. Med. Rep. 4, 105–111.
Yoshioka, H., Meno, C., Koshiba, K., Sugihara, M., Itoh, H., Ishimaru, Y., Inoue, T., Ohuchi, H., Semina, E.V., Murray, J.C., Hamada, H., Noji, S., 1998. Pitx2, a bicoid-type homeobox gene, is involved in a lefty-signaling pathway in determination of left–right asymmetry. Cell 94, 299–305.
Zhou, A.X., Hartwig, J.H., Akyurek, L.M., 2010. Filamins in cell signaling, transcription and organ development. Trends Cell Biol. 20, 113–123.